

**REPUBLIC OF TURKEY  
YILDIZ TECHNICAL UNIVERSITY  
GRADUATE SCHOOL OF NATURAL AND APPLIED SCIENCES**

**SPECTROSCOPY OF CHARMED SIGMA AND LAMBDA  
BARYONS IN LATTICE QUANTUM CHROMODYNAMICS**



**FATİH İLGIN**

**M.Sc. THESIS  
DEPARTMENT OF PHYSICS  
PROGRAM OF PHYSICS**

**ADVISER  
ASSOC. PROF. DR. TAYLAN YETKİN**

**CO-ADVISER  
PROF. DR. GÜRAY ERKOL**

**İSTANBUL, 2017**

**REPUBLIC OF TURKEY**  
**YILDIZ TECHNICAL UNIVERSITY**  
**GRADUATE SCHOOL OF NATURAL AND APPLIED SCIENCES**

**SPECTROSCOPY OF CHARMED SIGMA AND LAMBDA BARYONS IN  
LATTICE QUANTUM CHROMODYNAMICS**

A thesis submitted by Fatih ILGIN in partial fulfillment of the requirements for the degree of **MASTER OF SCIENCE** is approved by the committee on 01.06.2017 in Department of Physics.

**Thesis Adviser**

Assoc. P rof. Dr. T aylan YETKİN  
Yıldız Technical University

**Thesis Co-Adviser**

Prof. Dr. Güray ERKOL  
Özyeğin University

**Approved by the Examining Committee**

Assoc. Prof. Dr. Taylan YETKİN  
Yıldız Technical University

---

Assoc. Prof. Dr. Kutsal BOZKURT  
Yıldız Technical University

---

Assist. Prof. Dr. Bora IŞILDAK  
Özyeğin University

---



This study was supported by The Scientific and Technological Research Council of Turkey (TÜBİTAK) under project number 114F261.

## ACKNOWLEDGMENTS

---

It would not have been possible to complete of this work without support of my co-advisor, Güray ERKOL. I can not imagine having achieved this work without him. I would like to extend my special thanks to my advisor Taylan YETKİN. I can not recommend strongly enough that one take lessons from this great teacher.

I want to thank Assoc. Prof. Dr. Kutsal BOZKURT and Assist. Prof. Dr. Bora IŞILDAK to be a member of my jury. The sincerest thanks are for those four people for being so supportive and kind.

I would also like to thank Dr. Hüseyin DAĞ and Dr. Alper HAYRETER from Özyeğin University for their wise guidance and tireless help.

I want to thank specially Hüseyin BAHTİYAR for his great helps and supports along this work. More thanks to my friends Onur KARAYALÇIN and Utku CAN who supported me when I need. And all of my other friends whose companion I have always enjoyed.

Also, I want to thank PACS-CS collaboration for gauge configurations that we used for mass spectrum calculations.

Finally, I want to thank to my family, especially my mom and my wife, for their never ending support and love.

May, 2017

Fatih ILGIN

## TABLE OF CONTENTS

---

	Page
LIST OF SYMBOLS .....	vi
LIST OF ABBREVIATIONS .....	vii
LIST OF FIGURES .....	ix
LIST OF TABLES .....	ix
ABSTRACT .....	x
ÖZET .....	xi
CHAPTER 1	
INTRODUCTION .....	1
1.1 Literature Review .....	1
1.2 Objective of the Thesis .....	2
1.3 Hypothesis .....	3
CHAPTER 2	
LATTICE QCD .....	6
2.1 Path Integral on the Lattice .....	6
2.2 Naive Discretization for Space-time .....	7
2.2.1 Fermion Action .....	10
2.2.2 The Gluon Action .....	11
CHAPTER 3	
HADRON SPECTROSCOPY .....	15
3.1 Hadron Interpolators and Correlators .....	15
3.1.1 Meson Interpolators .....	16
3.1.2 Meson Correlators .....	18
3.1.3 Baryon Interpolators and Correlators .....	19
3.2 Extracting Hadron Masses .....	21

3.2.1	Techniques for Analyzing Data .....	22
3.3	Simulation Details.....	22
3.4	Chiral Extrapolation.....	23
3.5	Charmed Baryons .....	24
CHAPTER 4		
MASS SPECTRUM AND RESULTS .....		29
4.1	Mass Spectrum.....	29
CHAPTER 5		
RESULTS AND DISCUSSION .....		38
REFERENCES .....		40
CURRICULUM VITAE .....		42

## LIST OF ABBREVIATIONS

---

$\chi$ PT	Chiral Perturbation Theory
LQCD	Lattice Quantum Chromodynamics
QCD	Quantum Chromodynamics
QCDSR	Quantum Chromodynamics Sum Rules
QED	Quantum Electrodynamics
SM	Standard Model

## List of Figures

	Page
Figure 1.1 Strong coupling constant ( $\alpha_s$ ) as a function of momentum transfer [1]. ..	4
Figure 1.2 Lattice QCD results of hadron spectroscopy. (Points show lattice results and lines are experimental results) [2] .....	5
Figure 2.1 Link variables [3]. .....	11
Figure 2.2 The Plaquette $U_{\mu\nu}(n)$ is constructed by four Link variables [3].....	12
Figure 3.1 Multiplet for baryon octet and singlet ( $\Lambda^0$ ) [2]. .....	24
Figure 3.2 Multiplet for $s^{-\frac{3}{2}}$ baryon decuplet [5].....	25
Figure 3.3 Experimentally observed charmed baryons and decay channels [5]. .....	26
Figure 3.4 $SU(4)$ 20-plet for $s^{-\frac{1}{2}}$ [5].....	27
Figure 3.5 $SU(4)$ 4-plet for $s^{-\frac{1}{2}}$ [5].....	27
Figure 3.6 $SU(4)$ 20-plet for $s^{-\frac{3}{2}}$ [5].....	28
Figure 4.1 Effective mass vs. time graph of $\Lambda_c$ for $\kappa = 0.13700$ .....	30
Figure 4.2 Effective mass vs. time graph of $\Lambda_c$ for $\kappa = 0.13727$ .....	31
Figure 4.3 Effective mass vs. time graph of $\Lambda_c$ for $\kappa = 0.13754$ .....	31
Figure 4.4 Effective mass vs. time graph of $\Lambda_c$ for $\kappa = 0.13770$ .....	32
Figure 4.5 Effective mass vs. time graph of $\Sigma_c$ for $\kappa = 0.13700$ .....	33
Figure 4.6 Effective mass vs. time graph of $\Sigma_c$ for $\kappa = 0.13727$ .....	34
Figure 4.7 Effective mass vs. time graph of $\Sigma_c$ for $\kappa = 0.13754$ .....	35
Figure 4.8 Effective mass vs. time graph of $\Sigma_c$ for $\kappa = 0.13770$ .....	35

## LIST OF TABLES

		Page
Table 1.1	Elementary Particles [4]. .....	1
Table 1.2	Fundamental Forces of increasing strength [4]. .....	2
Table 3.1	Quantum numbers of the most commonly used meson interpolators according to the general form [2]. .....	18
Table 3.2	Interpolators for $s\text{-}\frac{1}{2}$ baryons. ....	20
Table 3.3	The details of the gauge configurations used in this work for $\Lambda_c$ and $\Sigma_c$ [5]. $N_s$ and $N_t$ are spatial and time components of the lattice, $N_f$ is the number of flavors, $L$ is volume of the lattice, $a$ is the lattice spacing, $\kappa_{val}^{u,d}$ is hopping parameter with flavor $u$ and $d$ , $N_{gc}$ is number of gauge configurations. ....	23
Table 3.4	Interpolating fields for $\Lambda_c$ and $\Sigma_c$ baryons. $C$ denotes charge conjugation matrix [6]. .....	27
Table 4.1	The effective mass values for baryons in questions ( $\Lambda_c$ ) for four different light quark hopping parameter values .....	32
Table 4.2	Extrapolated values to chiral limit ( $m_\pi^2 \rightarrow 0$ ) and compared values with other collaborations for $\Lambda_c$ .....	32
Table 4.3	The effective mass values for baryons in questions ( $\Sigma_c$ ) for four different light quark hopping parameters .....	36
Table 4.4	Extrapolated values to chiral limit ( $m_\pi^2 \rightarrow 0$ ) and compared values with other collaborations for $\Sigma_c$ .....	36
Table 4.5	Linear and quadratic extrapolation values.....	36
Table 4.6	Linear and quadratic extrapolation values.....	37

## ABSTRACT

---

### SPECTROSCOPY OF CHARMED SIGMA AND LAMBDA BARYONS IN LATTICE QUANTUM CHROMODYNAMICS

Fatih ILGIN

Department of Physics

M.Sc. Thesis

Adviser: Assoc. Prof. Dr. Taylan YETKİN

Co-Adviser: Prof. Dr. Güray ERKOL

Quantum Chromodynamics (QCD) is the theory of strong forces. In low-energy regions we need non-perturbative methods to study hadron properties.

Lattice QCD is a numerical and non-perturbative approach to QCD. This method is formulated on a 4-D discretized Euclidean space-time and starts directly from the QCD Lagrangian .

In this thesis, we have used  $32^3 \times 64$  and  $2 + 1$  flavor lattices to calculate the effective mass values for  $\Lambda_c$  and  $\Sigma_c$  baryons which are in agreement with experimental result and with those of other collaborations.

**Keywords:** QCD, lattice qcd, effective mass spectrum,  $\Lambda_c$  and  $\Sigma_c$  baryons.

---

YILDIZ TECHNICAL UNIVERSITY  
GRADUATE SCHOOL OF NATURAL AND APPLIED SCIENCES

### TILSIMLI LAMDA VE SİGMA BARYONLARININ ÖRGÜ KUANTUM RENK DİNAMİĞİNDE KÜTLE HESABI

Fatih ILGIN

Fizik Anabilim Dalı

Yüksek Lisans Tezi

Tez danışmanı: Assoc. Prof. Dr. Taylan YETKİN

Tez eş-danışmanı: Prof. Dr. Güray ERKOL

Kuantum Renk Dinamiği (KRD) güçlü nükleer etkileşimleri açıklayan bir teoridir. Ayrıca düşük enerjili durumlarda hadronlarla çalışabilmek için pertürbatif olmayan yöntemlere ihtiyacımız vardır.

Örgü KRD ise pertürbatif olmayan ve nümerik bir KRD çözüm yöntemidir. Bu yöntem dört boyutlu kesikli Öklit uzay zamanında tanımlanmıştır. Bu yöntemde hesaplamalar KRD Lagrangian'ından başlar.

Bu tezde,  $32^3 \times 64$  ve  $2 + 1$  çeşnili örgüler kullanarak,  $\Lambda_c$  ve  $\Sigma_c$  baryonlarının efektif kütlelerini, deney sonuçlarıyla uyumlu şekilde bulduk.

**Anahtar Kelimeler:** Örgü krd, efektif kütle spektrumu,  $\Lambda_c$  ve  $\Sigma_c$  baryonları.

INTRODUCTION

1.1 Literature Review

In Elementary Particle Physics, particles are classified in two different groups. These are *fermions* which have half-integer spin quantum number ( $s = 1/2, 3/2$ ), obeying Fermi-Dirac statistics, and *bosons* which have integer spin quantum number ( $s = 0, 1, 2$ ) and obeying Bose-Einstein statistics.

Fermions are classified in three quark families, three lepton subsegments or families which have six members and their corresponding anti-particles. Quarks are named as *up, down, charm, strange, top, bottom* (respectively  $u, d, c, s, t, b$ ) and leptons are named as *electron, muon, tau* and corresponding neutrinos ( $e, \mu, \tau, \nu_e, \nu_\mu, \nu_\tau$ ). They can be observed as an elementary particle or a composite particle which are named as hadron where *baryons* have three quarks and *mesons* have a quark-antiquark content.

Bosons can be observed as elementary particles (i.e.gauge bosons: photon, gluon,  $W^\pm, Z^0$  or scalar boson : Higgs boson) or a composite particle as mesons which belong to hadron family, having a quark and anti-quark couple(i.e.pseudoscalar mesons:  $\pi, K, D$  or vector mesons:  $\rho, \omega, \psi$ ).

In addition to these, we can identify some quantum numbers for elementary or composite particles to separate them from each other. All fermions and bosons have quantum num-

Table 1.1 Elementary Particles [4].

u	c	t	g	H
d	s	b	$\gamma$	
e	$\mu$	$\tau$	Z	
$\nu_e$	$\nu_\mu$	$\nu_\tau$	$W^\pm$	

bers. Some of these are electric charge, spin, isospin, parity, C parity, hypercharge, lepton number, baryon number, angular momentum and color charge. We can understand from these quantum numbers the interaction type. For example, all quarks and gluons have a color charge. It means that quarks and gluons interact strongly with each other. Because of that interaction we get a new property : colorlessness. We name these colorless objects as hadrons and classify them with respect to their quark content as baryons which have three quark and mesons which have one quark-antiquark pair.

## 1.2 Objective of the Thesis

In nature, there are four fundamental forces. They are electromagnetic force, weak nuclear force, strong nuclear force and gravitational force. Electromagnetic and gravitational forces have an infinitely long range as their mediators are photon and graviton. But gravitational force is a negligible force at atomic scale. In this section we will consider only other three forces.

Force	Theory	Mediator	Strength
Gravitational	Geometrodynamics	Graviton	$10^{-42}$
Weak	Flavordynamics	$W^\pm$ and $Z^0$	$10^{-13}$
Electromagnetic	Electrodynamics	Photon	$10^{-2}$
Strong	Chromodynamics	Gluon	10

Table 1.2 Fundamental Forces of increasing strength [4].

Electromagnetic force acts between electrically charged particles and it is the most observed force in daily life. Before Maxwell, electric and magnetic forces were accepted as different forces. But they have been unified as electromagnetic force by Maxwell. In particle physics, a theory has been developed called Quantum Electro Dynamics (QED) as well. It is Relativistic Quantum Field Theory of electrodynamics. Actually it explains how matter and photon interact. It is constructed on U(1) Abelian gauge group.

The Weak nuclear force or interaction helps us understand the nuclear  $\beta$  decay. As the name suggests, it takes place in nucleus of atom and has a small range. Moreover this force changes the flavor of quarks. From this perspective, this interaction is named as flavor dynamics as well. For weak interactions mediator particles are  $W^\pm$  and  $Z^0$  bosons.

In 1968, electromagnetic and weak forces were unified by Glashow, Salam and Weinberg and this unified force has been named as electro-weak force [4].

Strong nuclear force led by color charge can be seen as quark-quark, quark-gluon or gluon-gluon interaction. Because of the strong interaction, protons and nucleons are confined in nucleus of atom. But the range of this interaction is so short (it is equal to radius of nucleus, 1fm) compared to electromagnetic force, and energy scale for this interaction is about 1 GeV. The mediator particle for strong interaction is *gluon*. They are vector bosons whose spin quantum number is one ( $s = 1$ ) [4]. Gluons have color charge, too. It means that gluons can interact with each other strongly.

Standard Model is constructed on gauge groups  $SU(3) \times SU(2) \times U(1)$ . Here  $SU(n)$  denotes Special Unitary  $n \times n$  matrices. A special matrix whose determinant is unity and Unitary matrix means that its inverse is equal to its Hermitian conjugate.

$SU(2) \times U(1)$  correspond to the electroweak interaction in Standard Model.  $SU(3)$  is related to Quantum Chromodynamics (QCD) and generates strong interactions. QCD is a non-abelian theory.

With the advent of new types of observation techniques and sensor technology, after the mid fifties, plenty of hadrons have been observed. But it was understood that hadrons are not elementary particles. Although scientists have observed leptons and bosons, any free quark and gluon have not been observed so far. This is because all quarks and gluons have a color charge (have three different values) except spin and electric charge quantum number, differently from leptons.

### 1.3 Hypothesis

To understand the strong interaction, firstly we should explain strong coupling constant's behavior [7]. If we look at the Figure 1.1, we can see that in high energy vicinity (momentum transfer  $Q \rightarrow \infty$ ), strong coupling constant goes to zero. This behavior is named as *asymptotic freedom*. It means that there is not any interaction between quarks and gluons in this high energy regime. To be more precise, if there is a high energy reaction, quarks and gluons interact with weak force and they create a quark gluon plasma.

Another specific property native to QCD is *confinement*. It denotes that when you apply a force to separate two quarks, another quark-antiquark pair would be created. It means a free quark will never be observed.

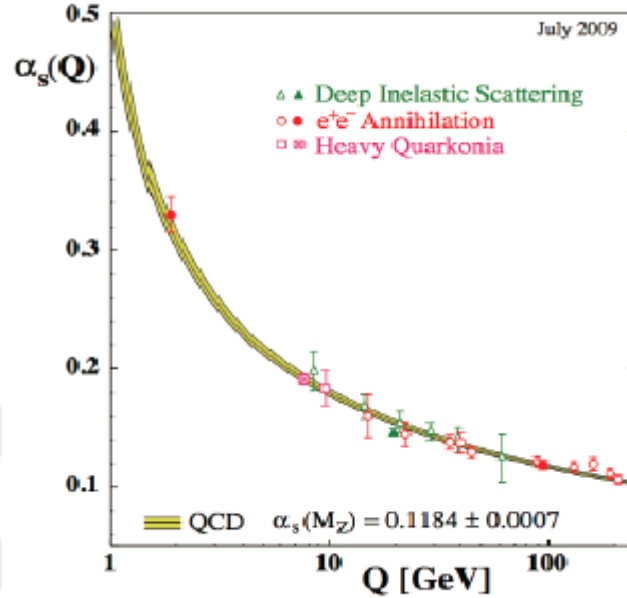


Figure 1.1 Strong coupling constant ( $\alpha_s$ ) as a function of momentum transfer [1].

According to the Figure 1.1, at small  $Q$  value, strong coupling constant has large values. So, perturbation theory breaks down in this vicinity. So if we study low-energy region, we need a non-perturbative procedure to understand the hadron structure [8, 9]. We have various non-perturbative methods which have been developed to probe the Hadron structure, for instance QCD Sum Rules (QCDSR) [10, 11], Chiral Perturbation Theory ( $\chi$ PT) [12, 13] and Lattice QCD (LQCD) [14, 15, 16].

In this thesis, we use Lattice QCD which is a promising non-perturbative method. For this method, we need a starting point. It is QCD Lagrangian which we need to model the strong interactions in 4D discretized Euclidean space-time:

$$\mathcal{L}_{QCD} = \bar{\psi}_i (i(\gamma^\mu D_\mu)_{ij} - m\delta_{ij}) \psi_j - \frac{1}{4} G_{\mu\nu}^\alpha G_{\alpha}^{\mu\nu}, \quad (1.1)$$

where  $\psi_i$  denotes quark field,  $A_\mu$  is gluon field,  $\gamma_\mu$  is Dirac matrix, and  $G_{\mu\nu}^\alpha$  represents

gluon field strength tensor. The Gluonic Strength tensor is given as

$$G_{\mu\nu}^{\alpha} = \partial_{\mu}A_{\nu}^{\alpha} - \partial_{\nu}A_{\mu}^{\alpha} + gf^{abc}A_{\mu}^bA_{\nu}^c. \quad (1.2)$$

Here  $f^{abc}$  denotes structure constant.

Lattice QCD method has been so successful to understand running coupling constant's behaviour and to calculate the spectroscopy of hadrons accurately. The spectrum results are consistent with experiments as shown in Figure 1.2.

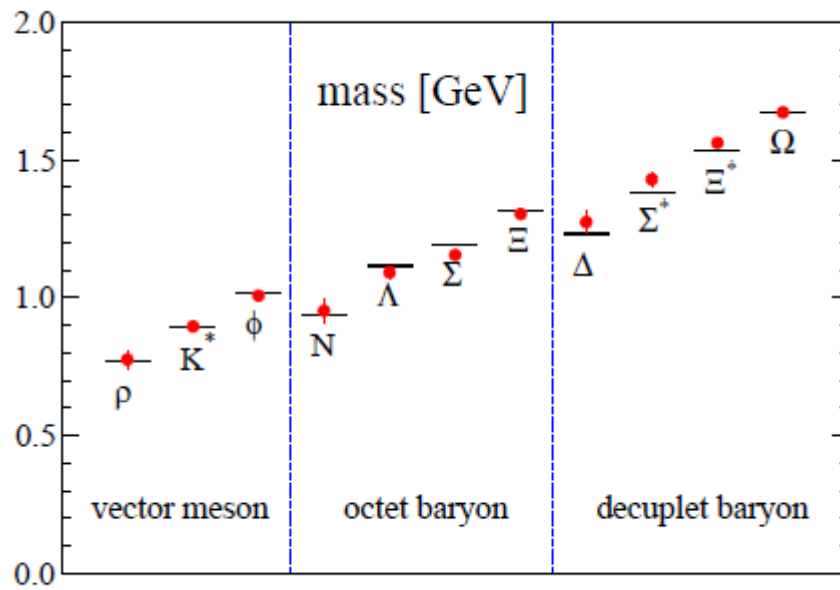


Figure 1.2 Lattice QCD results of hadron spectroscopy. (Points show lattice results and lines are experimental results) [2]

## CHAPTER 2

---

### LATTICE QCD

Quantum Chromo Dynamics is a formulation of strong interactions in terms of quarks and gluons. As we mentioned in Chapter 1, we are interested in Hadronic scale ( $\sim 1$  GeV). So perturbative methods are not applicable in this regime ( $\alpha_s \sim 1$ ). At low energy vicinity, lattice QCD is the only non-perturbative method that starts directly from the QCD lagrangian. In this section we summarize the method of lattice QCD.

#### 2.1 Path Integral on the Lattice

This section is dedicated to explaining the path integral formalism and we will use Gattringer-Lang notation [3]. Here Euclidean path integral is used to create quantized fields. Path integral will be introduced simply and two basic equations for lattice will be derived. First basic equation is

$$\lim_{T \rightarrow \infty} \frac{1}{Z_T} \langle O_2(t) O_1(0) \rangle_T = \sum_n \langle 0 | \hat{O}_2 | n \rangle \langle n | \hat{O}_1 | 0 \rangle e^{-tE_n}. \quad (2.1)$$

We can see here summation of exponents and each of them corresponds to an energy level. Here  $Z_T$  denotes the normalization factor. It is given with

$$Z_T = \text{tr}[e^{-T\hat{H}}]. \quad (2.2)$$

Left part of (2.1) is the Euclidean correlator for  $\hat{O}_1$  and  $\hat{O}_2$  operators,  $\hat{H}$  denotes the Hamiltonian for system. The right hand side in Euclidean correlator is given as a summation on

eigenstates of Hamiltonian operators tagged with  $n$ . In this summation there are matrix elements of  $\widehat{O}_i$  operators between vacuum state  $|0\rangle$  and any physical state  $|n\rangle$ . Moreover there is a weight factor on the right side,  $e^{-tE_n}$ , which contains the energy eigenvalues  $E_n$  for system [3]. It can be written in path integral form

$$\langle \widehat{O}_2(t)\widehat{O}_1(0) \rangle = \frac{1}{Z_T} \int D[\psi] e^{-S_e[\psi]} \mathcal{O}_2[\psi(\vec{x}, t)] \mathcal{O}_1[\psi(\vec{x}, 0)]. \quad (2.3)$$

Here  $\widehat{O}_2(t)$  and  $\widehat{O}_1(0)$  denote the Euclidean operators,  $E_n$  is the hadronic energy state,  $S_E[\psi]$  is the discretized action. On the right hand side, there is an integral over all probable forms of  $\psi$ .  $S_E$  denotes Euclidean action and  $Z_T$  is the partition function [21]

$$Z_T = \int D[\psi] e^{-S_e[\psi]}. \quad (2.4)$$

$\widehat{O}_1(0)$  is an operator which creates a particle from vacuum state  $|0\rangle$  and another  $\widehat{O}_2(t)$  operator annihilates this particle at time  $t$ . So, it can be said that for an hadronic state there is a creation-annihilation loop on lattice. Here we apply a trick called, named as Wick rotation, to solve correlation function numerically. So we transform our correlation function from Hilbert space to Euclidean space.

By doing Wick rotation from real time to an imaginary time  $t \rightarrow i\tau$ , we can get two important advantages. Firstly, weight factor  $e^{-S_E}$  does not sharply oscillate in Euclidean space, secondly by doing this rotation we can make use of similarities between *quantum field theories* and *statistical field theories*. This trick gives some advantages to use *statistical techniques* such as *Monte Carlo method* where weight factor transforms to  $e^{S_E}$ .

In following section we try to understand and discuss *the naive discretization of fermions*, *Wilson gauge action* and enhanced discretization techniques.

## 2.2 Naive Discretization for Space-time

In this part, we utilize Gattringer-Lang notation [3] and present discretization of space and time. Firstly, continuum space-time will be put in place with  $4D$  discrete lattice space-time.  $\Lambda$  denotes  $4D$  lattice space

$$\Lambda = \{n = (n_1, n_2, n_3, n_4) | n_1, n_2, n_3 = 0, 1, 2, 3, \dots, N-1; n_4 = 0, 1, 2, \dots, N_t-1\}.$$

Here  $N_T$  denotes time steps,  $N$  denotes all the spatial steps and  $n \in \Lambda$  shows positions in space time separated by lattice constant  $a$ .

In our discrete space-time, now we have *spinors* located at these lattice points, and they represent our fermionic particles as

$$\psi^f(x)_{\alpha c}, \quad \bar{\psi}^f(x)_{\alpha c}, \quad n \in \Lambda. \quad (2.5)$$

Here  $x$  denotes space-time, Dirac indices are denoted by  $\alpha = 1, 2, 3, 4$  color indices by  $c = 1, 2, 3$  (red, green, blue) and flavor indices by  $f$  which give quark's flavor (up, down, charm, strange, top, bottom). So, each spinor  $\psi^f(x)$  has 12 constituents. For notational convenience, we use  $n$  for lattice position of fermions, and it corresponds to real space-time position  $x = an$ . Here  $a$  is lattice spacing. But we generally drop it for clarity.

Furthermore, gauge fields for gluons are denoted by

$$A_\mu(x)_{cd}. \quad (2.6)$$

Here  $x$  is again space-time argument such in fermions,  $c, d = 1, 2, 3$  denote color index and  $\mu$  ( $\mu = 1, 2, 3, 4$ ) is Lorentz index. Also this  $A_\mu(x)$  field is a traceless and hermitian  $3 \times 3$  matrix.

In continuum space  $A_\mu$  is used to show the gauge fields, but on the lattice we would rather use *Link variables*  $U_\mu$  than  $A_\mu$ . Moreover there is an exponential relation between continuum gauge field  $A_\mu$  and  $U_\mu$  [2],

$$U_\mu(n) = \exp(iaA_\mu(n)). \quad (2.7)$$

These link variables make a connection between the lattice points. It is convenient to separate the continuum or discrete QCD action into a fermionic part and a gluonic part.

Fermionic part contains quark fields and interaction term. Gluonic part defines propagation and interaction between the gluons.

We try to simulate infinite space time with finite discretized space time. Therefore, we confront some problem on this process about boundaries. For this purpose we choose periodic boundary conditions to conserve the symmetry.

We write continuum QCD action firstly. Then we will separate it two part as fermionic and gluonic action in continuum QCD. Secondly, we discretize the space and time. In continuum space, QCD action is given as

$$S[\psi, \bar{\psi}, A] = \sum_{n=1}^{N_f} \int d^4x \bar{\psi}^f(x)_{\alpha c} [\not{\partial} + ig\not{A}(x) + m^{(f)}] \psi^{(f)}(x)_{\alpha c} + \frac{1}{2} \int d^4x \text{Tr}[F_{\mu\nu} F^{\mu\nu}]. \quad (2.8)$$

Here individually  $\psi^{(f)}(x)_{\alpha c}$  and  $\bar{\psi}^{(f)}(x)_{\alpha c}$  denotes Dirac spinors for fermions and anti-fermions,  $\alpha$  denotes Dirac index,  $c$  and  $d$  denote color indices.  $\not{A}$  and  $\not{\partial}$  show the Feynman slash notation and it is related to gauge field and derivative by a gamma matrix multiplication

$$\not{A} = \gamma^\mu A_\mu, \quad (2.9)$$

$$\not{\partial} = \gamma^\mu \partial_\mu. \quad (2.10)$$

Here,  $A_\mu$  denotes gauge field,  $g$  is strong coupling constant and  $F_{\mu\nu}$  gives Field strength tensor

$$F_{\mu\nu} = \partial_\mu A_\nu(x) - \partial_\nu A_\mu(x) + ig[A_\mu, A_\nu]. \quad (2.11)$$

If we write the gauge field with color components

$$A_\mu(x) = \sum_{i=1}^8 A_\mu^i(x) T_i. \quad (2.12)$$

By using this information about gauge field, we can write again field strength tensor as

$$F_{\mu\nu}(x) = \sum_{i=1}^8 \{ \partial_\mu A_\nu^i(x) - \partial_\nu A_\mu^i(x) - gf_{jki} A_\mu^j A_\nu^k \} T_i. \quad (2.13)$$

Here  $T_i$  denotes Gell-Mann matrices and  $f_{jki}$  indicates structure constant. Finally, we can write the QCD action again as follows

$$S[\psi, \bar{\psi}, A] = \sum_{n=1}^{N_f} \int d^4x \bar{\psi}^f(x)_{\alpha c} [\not{\partial} + ig\not{A}(x) + m^{(f)}] \psi^{(f)}(x)_{\alpha c} - \frac{1}{4} \sum_{i=1}^8 \int d^4x F_{\mu\nu}^i(x) F_i^{\mu\nu}(x). \quad (2.14)$$

The indices are written here clearly and it can be seen that there are eight combinations for gluons.

We now separate the fermionic and gluonic action.

### 2.2.1 Fermion Action

For a free fermion ( $A_\mu=0$ ), in continuum space, the action  $S_F^0$  is given as

$$S_F^0[\psi, \bar{\psi}] = \int d^4x \bar{\psi}(x) (\gamma_\mu \partial_\mu + m) \psi(x). \quad (2.15)$$

In this action, the space-time integral and derivative have to be discretized. This discretization is executed as a summation upon  $\Lambda$ . Firstly, we show how the partial derivative is discretized as

$$\partial_\mu \psi_\mu(x) \rightarrow \frac{1}{2a} (\psi(n+\mu) - \psi(n-\mu)). \quad (2.16)$$

So, in discrete space-time, our free fermionic particle's action in lattice becomes

$$S_F^0[\psi, \bar{\psi}] = a^4 \sum_{n \in \Lambda} \bar{\psi}(n) \left( \sum_{\mu=1}^4 \gamma_\mu \frac{\psi(n+\mu) - \psi(n-\mu)}{2a} + m\psi(n) \right). \quad (2.17)$$

From this equation, we can see whether this action is gauge invariant or not under SU(3) gauge transformations

$$\psi(n) \rightarrow \psi'(n) = \Omega(n)\psi(n), \quad (2.18)$$

$$\bar{\psi}(n) \rightarrow \bar{\psi}'(n) = \bar{\psi}(n)\Omega^\dagger(n). \quad (2.19)$$

Here  $\Omega(n)$  denotes a phase in SU(3) gauge. Similarly if we try to do gauge transformation on link variables

$$U_\mu(n) \rightarrow U'_\mu(n) = \Omega(n)U_\mu(n)\Omega^\dagger(n+\mu). \quad (2.20)$$

Finally we can get a gauge invariant fermionic action by using these transformation

$$S_F[\bar{\psi}, \psi, U] = a^4 \sum_{n \in \Lambda} \bar{\psi}(n) \left[ \sum_{\mu=1}^4 \gamma_\mu \frac{U_\mu(n)\psi_\mu(n+\mu) - U_\mu^\dagger(n-\mu)\psi(n-\mu)}{2a} + m\psi(n) \right]. \quad (2.21)$$

### 2.2.2 The Gluon Action

In this section, we show how to discretize the gauge action. For this process we introduce a gauge invariant object. It is called *Link variable* ( $U_\mu(n)$ ) which makes a connection between lattice points  $n$ . It connects lattice point  $n$  to  $n + \mu$ .

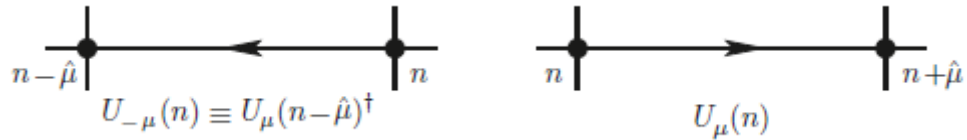


Figure 2.1 Link variables [3].

As shown in figure 2.1,  $U_\mu(n)$  corresponds to link variable from  $n$  to  $n + \mu$  and  $U_{-\mu}(n)$

corresponds the link variable from  $n$  to  $n - \mu$ . We also have

$$U_{-\mu}^\dagger(n - \mu) \equiv U_{-\mu}(n). \quad (2.22)$$

Morover, it is important to define the shortest and closed loop of link variables on the lattice. It is called *plaquette*. By using four *Link variables* we create a plaquette variable  $U_{\mu\nu}(n)$  as shown in figure 2.2.

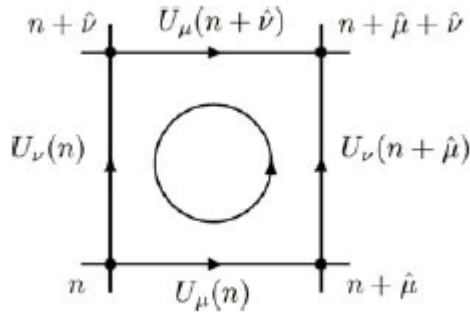


Figure 2.2 The Plaquette  $U_{\mu\nu}(n)$  is constructed by four Link variables [3].

$$U_{\mu\nu}(n) = U_{\mu}(n)U_{\nu}(n + \mu)U_{-\mu}(n + \nu + \mu)U_{-\nu}(n + \nu). \quad (2.23)$$

Equivalently, we can write again this equation by using Eq. 2.22

$$U_{\mu\nu}(n) = U_{\mu}(n)U_{\nu}(n + \mu)U_{\mu}^\dagger(n + \nu)U_{\nu}^\dagger(n). \quad (2.24)$$

After this introduction of plaquette, we can define Wilson gauge action which is formulated firstly in lattice gauge theory and after that we show how to approach the continuum limit ( $a \rightarrow 0$ ). The Wilson gauge action can be calculated by doing a summation over all plaquettes. We can do this summation over all lattice points  $n$  which are located on plaquettes [3]. So, our Wilson gauge action is

$$S_G[U] = \frac{\beta}{3} \sum_{n \in \Lambda} \sum_{\mu < \nu} \text{ReTr}[1 - U_{\mu\nu}(n)]. \quad (2.25)$$

This summation is made over Lorentz indices  $\mu$  and  $\nu$

$$1 \leq \mu < \nu \leq 4. \quad (2.26)$$

In this equation,  $\beta$  denotes the lattice coupling and there is an inverse proportion between strong coupling and lattice coupling,  $\beta = \frac{6}{g^2}$ . In continuum limit  $a \rightarrow 0$ , wilson gauge action would be equal to the gauge action in continuum space:

$$S_G[A] = \frac{1}{2g^2} \int d^4x Tr[F_{\mu\nu}(x)F_{\mu\nu}(x)]. \quad (2.27)$$

If we want to extend the link variables for small lattice spacing values in Eq. 2.9, we come across a limit problem. To overcome this problem we use Baker Campel Housedorf formulation for product of exponentials of matrices

$$\exp(A)\exp(B) = \exp\left(A + B + \frac{1}{2}[A, B] + \dots\right). \quad (2.28)$$

Here A and B are random matrices, and if we insert Eq. 2.25 to Eq. 2.9 and Eq. 2.25, we get a new iterative plaquette equation:

$$\begin{aligned} U_{\mu\nu}(n) = & \exp\left(iaA_\mu(n) + iaA_\nu(n + \hat{\mu}) - \frac{a^2}{2}[A_\mu(n), A_\nu(n + \mu)]\right. \\ & - iaA_\mu(n + \hat{\nu}) - iaA_\nu(n) - \frac{a^2}{2}[A_\mu(n + \hat{\nu}), A_\nu(n)] \\ & + \frac{a^2}{2}[A_\nu(n + \hat{\mu}), A_\mu(n + \hat{\nu})] + \frac{a^2}{2}[A_\mu(n), A_\nu(n)] \\ & \left. + \frac{a^2}{2}[A_\mu(n), A_\nu(n + \hat{\nu})] + \frac{a^2}{2}[A_\nu(n + \hat{\mu}), A_\nu(n)] + \mathcal{O}(a^3)\right). \quad (2.29) \end{aligned}$$

In this equation, we have  $A_\mu$  gauge fields, and Taylor Expansion of this fields is

$$A_\nu(n + \hat{\mu}) = A_\nu(n) + a\partial_\mu A_\nu(n) + \mathcal{O}(a^2). \quad (2.30)$$

By using this expansion, many terms will be cancelled and we get the continuum plaquette equation

$$\begin{aligned} U_{\mu\nu}(n) = & \exp\left(ia^2(\partial_\mu A_\nu(n) - \partial_\nu A_\mu(n) + i[A_\mu(n), A_\nu(n)])\mathcal{O}(a^3)\right) \\ = & \exp\left(ia^2 F_{\mu\nu}(n) + \mathcal{O}(a^3)\right). \quad (2.31) \end{aligned}$$

Now we can use this form in Eq. 2.27, and by expanding the exponential term in Eq. 2.33, we get the continuum wilson gauge action equation

$$S_G[U] = \frac{2}{g^2} \sum_{n \in \Lambda} \sum_{\mu < \nu} \text{ReTr}[\mathbb{1} - U_{\mu\nu}(n)] = \frac{a^4}{2g^2} \sum_{n \in \Lambda} \sum_{\mu, \nu} \text{Tr}[F_{\mu\nu}^2(n)] + \mathcal{O}(a^2). \quad (2.32)$$

Thus we get a discretized QCD formula. It was formulated by K. Wilson in 1974 [14]. When we try to approach from a discretized action to continuum action, we are confronted with some errors. Although it seems that there are no errors when it is taken continuum limit  $a \rightarrow 0$ , in practice we cannot calculate with zero lattice spacing, so, there are always systematic errors.

Because of these systematic errors, some corrections are necessary. There are some different gauge actions to solve these error problems.

### HADRON SPECTROSCOPY

Because of the spin, parity, flavor, etc. quantum numbers and their combinations, there are many hadrons which we know. One of the basic quantities of hadrons that can be computed using Lattice QCD is their mass value. These mass values have been measured experimentally. So lattice calculations can be thought as complementary for QCD. We can achieve high precision in lattice calculations, and good agreement with experiment. In this chapter we introduce some basic knowledge about hadron spectroscopy calculations and hadron correlation function. Firstly we summarize operators and their correlation functions and then we show calculation methods for quark sources and propagators. Finally we analyze hadron propagators and show how to get hadron masses [2]. Interpolators could be defined as Euclidean correlators of hadron interpolators  $O(n_t)$  and  $\bar{O}(0)$ . For hadron spectroscopy calculations, first step is to understand the interpolators which are constructed with quarks and gluons.

#### 3.1 Hadron Interpolators and Correlators

Here we discuss how to carry out hadron spectroscopy calculations. So, firstly we compute quark propagators for all combinations. Then we use them to establish hadron propagators and we find an average value for all gauge configurations. So we can estimate the hadron propagators.

In spectroscopy calculations, firstly we should identify the hadron interpolators  $O$ ,  $\bar{O}$  which conform in Hilbert space to operators ( $\hat{O}$  and  $\hat{O}^\dagger$ ) for annihilation and creation of particles. By using these interpolators ( $O(n_t)$  and  $\bar{O}(0)$ ) placed at time slices  $n_4 = n_t$  and

$n_4 = 0$ , we get an Euclidean correlator of Hadron interpolators<sup>1</sup>

$$\langle O_2(t)O_1(0) \rangle_T = \frac{1}{Z_T} \text{Tr}[e^{(T-t)\hat{H}} \hat{O}_2 e^{-t\hat{H}} \hat{O}_1]. \quad (3.1)$$

The interpolators what we need for hadron spectroscopy which include quarks and gluons, are gauge invariant color singlets. For example, these interpolators or operators for mesons can be written as

$$O_M(n) \equiv \bar{\psi}(n)\Gamma\psi(n). \quad (3.2)$$

A meson has a quark and an antiquark and a baryon has three quarks. Moreover, we can extend this method to get exotic color singlet combinations of quarks and anti-quarks for tetraquark ( $\bar{\psi}\bar{\psi}\psi\psi$ ) and pentaquark ( $\bar{\psi}\psi\psi\psi\psi$ ). Extended interpolators involve terms like  $\bar{\psi}(n)U_\mu(n)\psi(n+\mu)$  for mesons. Similarly it can be extended for baryons.

If we want to find some physical observables, we do a spectral decomposition for propagators of interpolators

$$\begin{aligned} \langle O(n_t)\bar{O}(0) \rangle &= \sum_k \langle 0|\hat{O}|k \rangle \langle k|\hat{O}^\dagger|0 \rangle e^{-n_t a E_k} \\ &= A e^{-n_t a E_H} (1 + \mathcal{O}(e^{-n_t a \Delta E})) \end{aligned} \quad (3.3)$$

Here, A is a constant and  $E_H$  is a ground state energy for  $|H\rangle$  and  $\langle 0|\hat{O}|H\rangle \neq 0$  and  $\Delta E$  is the energy difference between ground state and first excited state. From this equation we can obtain energy  $E_H$  for hadrons.

### 3.1.1 Meson Interpolators

In this section we show how to create a meson interpolator and give *pion* as an example. Then we can extend this to other mesons. In this example, we know that a pion is constructed by an up and a down quark state. For up and down quarks, isospin ( $I$ ), isospin z-component ( $I_z$ ) and electrical charge values are respectively  $I = +\frac{1}{2}, +\frac{1}{2}$ ,  $I_z = +\frac{1}{2}, -\frac{1}{2}$  and  $Q = \frac{2}{3}e, -\frac{1}{3}e$ . If we take the charged pions,  $\pi^+$  and  $\pi^-$ , they have 138 MeV mass value and total spin is ( $J = 0$ ), parity is negative ( $P = -1$ ), isospin and isospin-z are

---

<sup>1</sup>We use "operator" and "interpolator" as equivalent words.

$I = +1$ ,  $I_z = \pm 1$  and charge  $Q = \pm 1$  again. By using these quantum numbers, we can estimate the content of  $\pi^\pm$ , so  $\pi^+ = u\bar{d}$  and  $\pi^- = \bar{u}d$  combinations. In the light of this information we can create meson interpolators

$$O_{\pi^+}(n) = \bar{d}(n)\gamma_5 u(n),$$

$$O_{\pi^-}(n) = \bar{u}(n)\gamma_5 d(n).$$

Under parity transformation we find that

$$\begin{aligned} O_{\pi^+}(\mathbf{n}, n_4) &= \bar{d}(\mathbf{n}, n_4)\gamma_5 u(\mathbf{n}, n_4) \\ \xrightarrow{\mathcal{P}} \bar{d}(-\mathbf{n}, n_4)\gamma_4\gamma_5\gamma_4 u(-\mathbf{n}, n_4) &= -\bar{d}(-\mathbf{n}, n_4)\gamma_5 u(-\mathbf{n}, n_4) \\ &= -O_{\pi^+}(-\mathbf{n}, n_4). \end{aligned}$$

This result shows that  $O_{\pi^+}$  interpolator has negative parity and parity operation transforms spatial vector  $\mathbf{n}$  to  $-\mathbf{n}$  and If we apply charge conjugation, it gives

$$\begin{aligned} O_{\pi^+}(n) = \bar{d}(n)\gamma_5 u(n) &\xrightarrow{\mathcal{C}} -d(n)^T C\gamma_5 C^{-1}\bar{u}(n)^T = -d(n)^T \gamma_5^T \bar{u}(n)^T \\ &= \bar{u}(n)\gamma_5 d(n) = O_{\pi^-}(n). \end{aligned}$$

Here,  $\mathcal{C}\gamma_5\mathcal{C}^{-1} = \gamma_5^T$ , so this equation shows how charge conjugation transforms  $O_{\pi^+}$  to  $O_{\pi^-}$  and vice versa.

For  $\pi^0$  which is  $I_z = 0$  component for iso-triplet

$$O_{\pi^0}(n) = \frac{1}{\sqrt{2}}(\bar{u}(n)\gamma_5 u(n) - \bar{d}(n)\gamma_5 d(n)). \quad (3.4)$$

Furthermore, we can extend these interpolator examples for  $\eta$  meson which is an iso-singlet state ( $I = 0$ )

$$O_\eta(n) = \frac{1}{\sqrt{2}}(\bar{u}(n)\gamma_5 u(n) + \bar{d}(n)\gamma_5 d(n)). \quad (3.5)$$

It could be seen easily here that the properties of  $O_{\pi^0}$  and  $O_\eta$  are the same under parity transformation like between interpolators  $O_{\pi^+}$  and  $O_{\pi^-}$ . That is, they have negative parity ( $P = -1$ ). But they have positive charge conjugation value ( $C = +1$ ). By using

Table 3.1, which shows quantum numbers, the other interpolators can be constructed in the same way.

State	$J^{PC}$	$\Gamma$	Particles
Scalar	$0^{++}$	$\mathbb{1}, \gamma_4$	$f_0, a_0, K_0^*$
Pseudoscalar	$0^{-+}$	$\gamma_5, \gamma_4 \gamma_5$	$\pi^\pm, \pi^0, \eta, K^\pm, K^0 \dots$
Vector	$1^{--}$	$\gamma_i, \gamma_4 \gamma_i$	$\rho^\pm, \rho^0, \omega, K^*, \phi \dots$
Axial vector	$1^{+-}$	$\gamma_i \gamma_5$	$a_1, f_1 \dots$
Tensor	$1^{+-}$	$\gamma_i \gamma_j$	$h_1, b_1 \dots$

Table 3.1 Quantum numbers of the most commonly used meson interpolators according to the general form [2].

Due to different flavor content, parity and spin, mesons have different interpolators. For example, we can model an interpolator for  $K^+$  meson on  $\pi^+$  meson by putting in place of  $d$  quark with  $s$  quark

$$O_{K^+}(n) = \bar{s}(n) \gamma_5 u(n). \quad (3.6)$$

Morover, if there are different spin or parity values, different gamma matrices must be used. For instance, we can get an interpolator for  $\rho^+$  vector meson ( $I = 1, I_z = +1, Q = +e, J = 1, P = -1$ ) from  $\pi^+$  meson's interpolator by replacing  $\gamma_5$  with  $\gamma_i, i = 1, 2, 3$

$$O_{\rho^+}(n)_i = \bar{d}(n) \gamma_i u(n), \quad i = 1, 2, 3. \quad (3.7)$$

Generally a meson interpolator can be defined

$$O_M(n) = \bar{\psi}^{(f_1)}(n) \Gamma \psi^{(f_2)}(n). \quad (3.8)$$

$\Gamma$  denotes the gamma matrices and  $f_i$  denotes flavor indices. In Table 2, most commonly used gamma matrices ( $\Gamma$ ) are listed for different interpolators with corresponding quantum numbers.

### 3.1.2 Meson Correlators

In the previous section we mention about euclidean correlator and interpolators. But now we should find hermitian conjugate of a meson interpolator  $\hat{\psi}_M^\dagger$  which create a meson

from vacuum state. If we take the hermitian conjugate of Eq. 3.3

$$(\bar{\psi}^{(f_1)}\Gamma\psi^{(f_2)})^\dagger = -\psi^{(f_2)}\Gamma^\dagger\psi^{(f_1)\dagger} = \pm\bar{\psi}^{(f_2)}\Gamma\psi^{(f_1)}. \quad (3.9)$$

Here is a minus sign because of Grassmann variables changing and there are some basic properties,  $\bar{\psi} = \psi^\dagger \gamma_4$  and  $\gamma_4\Gamma^\dagger\gamma_4 = \pm\Gamma$ . Finally we can write for meson interpolator on  $m, n$  spatial coordinates

$$O_M(n) = \bar{\psi}^{(f_1)}(n)\Gamma\psi^{(f_2)}(n),$$

$$O_M(n) = \bar{\psi}^{(f_1)}(m)\Gamma\psi^{(f_2)}(m).$$

By using this interpolator we create correlator  $\langle O_M(n)\bar{O}_M(m) \rangle$ . There is a distinction between for iso-triplet state correlator and iso-singlet state correlator. For an iso-triplet state, the interpolator is  $O_T = \bar{d}\Gamma u$ , and if we write all indices, we obtain

$$\begin{aligned} \langle O_T(n)\bar{O}_T(m) \rangle_F &= \langle \bar{d}(n)\Gamma u(n)\bar{u}(m)\Gamma d(m) \rangle_F \\ &= -Tr[\Gamma D_u^{-1}(n|m)\Gamma D_d^{-1}(m|n)]. \end{aligned}$$

Here  $D_u$  and  $D_d$  denotes Dirac operators. By neglecting the small differences of quark mass for  $u$  and  $d$ , we can get Dirac operators identical,  $D_u=D_d$ .

As a result, we interpret that propagators  $D_d^{-1}(m|n)$  propagate  $u$  and  $d$  quarks from  $m$  to  $n$  point. We can extend this calculation for iso-singlet and iso-triplet (for  $I_z = 0$ ) states' interpolators to obtain correlators.

### 3.1.3 Baryon Interpolators and Correlators

In this section, firstly we write an interpolator for nucleons. Then accordingly we can create for other baryons as we did for mesons in previous section. For example a proton and a neutron have respectively  $+\frac{1}{2}$  and  $-\frac{1}{2}$  isospin-z values. So they are iso-doublet states ( $I = \frac{1}{2}$ ). The proton is a  $uud$  state and neutron is a  $udd$  state and the simplest

interpolator for a  $uud$  type nucleon state is

$$O_N(n) = \varepsilon_{abc} u(n)_a (u(n)_b^T C \gamma_5 d(n)_c). \quad (3.10)$$

Here  $a, b, c$  denote the color indices,  $C$  corresponds to charge conjugation and  $T$  is the transpose. When we combine the  $u$  and the  $d$  quarks in parentheses with  $C$  and  $\gamma_5$ , we would create a *diquark* which has isospin  $I = 0$  and spin  $J = 0$  values.

Similarly we can write an interpolator for corresponding creation operator as follows

$$\bar{O}_{N_\pm}(n) = \varepsilon_{abc} (\bar{u}(n)_\alpha C \gamma_5 \bar{d}(n)_b^T) \bar{u}(n)_c P_\pm. \quad (3.11)$$

Here  $P_\pm$  denotes the parity projector which is

$$P_\pm = \frac{1}{2} (\mathbb{1} \pm \gamma_4). \quad (3.12)$$

In conclusion, we can extract a nucleon correlator by using these interpolators as noted below (we use  $P_\pm^2 = P_\pm$ )

$$\begin{aligned} \langle O_{N_\pm}(n)_\alpha \bar{O}_{N_\pm}(m)_\alpha \rangle_F &= \langle \bar{O}_{N_\pm}(m)_\alpha O_{N_\pm}(n)_\alpha \rangle_F \\ &= -\langle \varepsilon_{abc} \varepsilon_{a'b'c'} (\bar{u}(m)_\alpha C \gamma_5 \bar{d}(m)_b^T) \bar{u}(m)_c P_\pm u(n)_{c'} (u(n)_{\alpha'}^T C \gamma_5 d(n)_{b'}) \rangle_F \\ &= \varepsilon_{abc} \varepsilon_{a'b'c'} (C \gamma_5)_{\alpha' \beta'} (C \gamma_5)_{\alpha \beta} (P_\pm)_{\gamma \gamma'} D_d^{-1}(n|m)_{\beta \beta'} \times \\ &\quad (D(u)^{-1}(n|m)_{\alpha 2 \alpha} D(u)^{-1}_{\gamma' \gamma} - D(u)^{-1}(n|m)_{\alpha' \gamma} D(u)^{-1}(n|m)_{\gamma' \alpha}). \end{aligned}$$

For octet baryon's interpolating fields are given as in Table (3.2).

$O_{\Lambda_\pm} = \varepsilon_{abc} P_\pm \Gamma^A (2s_a [u_b^T \Gamma^B d_c] + (d_a [u_b^T \Gamma^B s_c]) - (u_a [d_b^T \Gamma^B s_c]))$
$O_{\Sigma_\pm} = \varepsilon_{abc} P_\pm \Gamma^A u_a [u_b^T \Gamma^B s_c]$
$O_{N_\pm} = \varepsilon_{abc} P_\pm \Gamma^A u_a [u_b^T \Gamma^B d_c]$
$O_{\Xi_\pm} = \varepsilon_{abc} P_\pm \Gamma^A s_a [s_b^T \Gamma^B u_c]$

Table 3.2 Interpolators for  $s\text{-}\frac{1}{2}$  baryons.

### 3.2 Extracting Hadron Masses

In this section, we present how to calculate the hadron masses by using correlators which we explained in previous sections. In hadron correlator formula

$$\begin{aligned} \langle O(n_t)\bar{O}(0) \rangle &= \sum_k \langle 0|\hat{O}|k\rangle \langle k|\hat{O}^\dagger|0\rangle \exp(-n_t a E_k) \\ &A \exp(-n_t a E_H) (1 + \mathcal{O}(\exp(-n_t a \Delta E))). \end{aligned}$$

Here we use *lattice constant* ( $a$ ) as a factor for energy, mass and momentum. So we get  $aE$ ,  $am$  and  $ap$  as dimensionless values. Moreover, we use operators  $\hat{O}^\dagger$  and  $\hat{O}$  for creation and annihilation respectively. Namely,  $\hat{O}^\dagger$  creates a hadron from vacuum and  $\hat{O}$  annihilates a hadron to vacuum state. If the annihilation or *sink* operator has zero momentum, we write again correlation function as

$$C(n_t) \equiv \langle \tilde{O}(\mathbf{0}, n_t)\bar{O}(\mathbf{0}, 0) \rangle = \sum_k \langle 0|\hat{O}|k\rangle \langle k|\hat{O}^\dagger|0\rangle e^{-n_t E_k}.$$

In this calculation, we use a finite lattice. So  $E_k$  has a discretized value. If operators are for a single particles, the mass value is equal to ground state energy ( $E_k = m_k$ ). But if there are two or more particle states, the energy values correspond to mass and momentum. Because of the exponential part of this equation, the relation can be seen between  $n_t$  values and energy states. That is, if we have large  $n_t$  values, the lowest energy states are dominant. On the contrary, for smaller  $n_t$  values,  $C(n_t)$  equation has many contributions

$$C(n_t) = A_0 e^{-n_t E_0} + A_1 e^{-n_t E_1} + \dots \quad (3.13)$$

By using these equations, we can extract an *effective mass* formula

$$m_{eff}(n_t + \frac{1}{2}) = \ln \frac{C(n_t)}{C(n_t + 1)}. \quad (3.14)$$

When  $m_{eff}$  has constant value, correlator  $C(n_t)$  is dominated by minimum energy state and graphic forms a plateau at  $m_{eff} = E_0$ .

### 3.2.1 Techniques for Analyzing Data

In order to process our data, we used Jackknife method. It is a simple method to determine the statistical errors of the fit results for the mass. This method is a resampling method and very useful for extinguishing bias parameters. Assume that for a data set with size  $N$  and  $\theta$  are observables. And there is a computed observable value for original data set is called  $\hat{\theta}$ . So the variance value for  $\theta$  is

$$\sigma_{\hat{\theta}}^2 = \frac{N-1}{N} \sum_{n=1}^N (\theta_n - \hat{\theta})^2. \quad (3.15)$$

For finding the standard deviation of  $\theta$ , we take the square root of this  $\theta$  value. So we can compute a bias estimator as  $\langle \theta \rangle = \hat{\theta} \pm \sigma_{\hat{\theta}}$ . Also the bias can be calculated from

$$\tilde{\theta} \equiv \frac{1}{N} \sum_{n=1}^N \theta_n, \quad (3.16)$$

which concludes to  $\tilde{\theta} - (N-1)(\tilde{\theta} - \hat{\theta})$  for the unbiased estimator for  $\langle \theta \rangle$ . By using Jackknife method determination the statistical errors for fitted quantity could be seen the most important advantage in data analysis.

### 3.3 Simulation Details

We examine mass spectrum of charmed baryon using relativistic heavy quark action in 2+1 flavor PAC-CS configurations which are formerly generated on  $32^3 \times 64$  lattice [5]. Details of configurations are given in Table 3.2. We have used four different sets of configurations for light quark hopping parameters  $\kappa_{sea}^{u,d} = 0.13700, 0.13727, 0.13754, 0.13770$  which conform to pion masses respectively 700, 570, 410, 300 MeV.

Table 3.3 The details of the gauge configurations used in this work for  $\Lambda_c$  and  $\Sigma_c$  [5].  $N_s$  and  $N_t$  are spatial and time components of the lattice,  $N_f$  is the number of flavors,  $L$  is volume of the lattice,  $a$  is the lattice spacing,  $\kappa_{val}^{u,d}$  is hopping parameter with flavor  $u$  and  $d$ ,  $N_{gc}$  is number of gauge configurations.

$N_s^3 \times N_t$	$N_f$	$a[\text{fm}]$	$a^{-1}[\text{GeV}]$	$L$ (fm)
$32^3 \times 64$	$2 + 1$	0.0907(13)	2.176(31)	2.90
$\kappa_{val}^{u,d}$	0.31700	0.13727	0.13754	0.13770
$N_{gc}$	100	100	199	316

### 3.4 Chiral Extrapolation

Because of technical issues in the discretization of the fermion action we cannot compute values at physical quark masses and we are forced to extrapolate our unphysical values to physical point (chiral point) to obtain a physical mass value ( $m_q \rightarrow 0$ ). So, we fit our data to a linear function

$$M_{eff} = a_1 + a_2(am_\pi)^2. \quad (3.17)$$

From this equation we can extract a fixed  $a_1$  value to extract an effective mass by extrapolating to the physical  $m_\pi$  value. Secondly we can fit them to a quadratic function as

$$m_{eff} = a_1 + a_2(am_\pi)^2 + a_3(am_\pi)^4.$$

Furthermore, there may be many sources of systematical errors from discretization. These are finite volume effect and chiral extrapolation. Except these systematical errors, there may be statistical errors from Monte Carlo sampling of observables. In order to get rid of these errors and bias, we have employed Jackknife resampling method.

### 3.5 Charmed Baryons

Charmed baryons that include at least one charm quark were observed firstly in 1970's. Recently, many new charmed baryon states were observed by BaBar, BELLE [17], CLEO [18] and LHCb [19] collaborations. We can classify the baryons according to spins and flavors. In Fig.(3.1) and Fig.(3.2), we can show  $s = \frac{1}{2}$  octet state  $8 \oplus 1$  and  $s = \frac{3}{2}$  decuplet states.

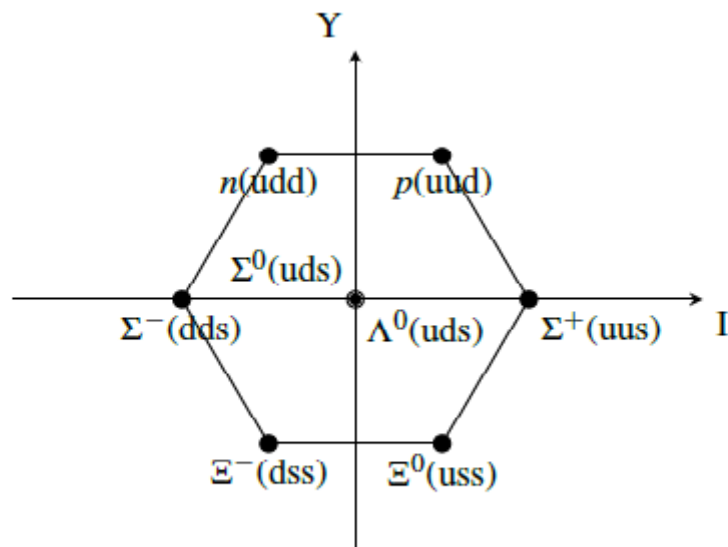


Figure 3.1 Multiplet for baryon octet and singlet ( $\Lambda^0$ ) [2].

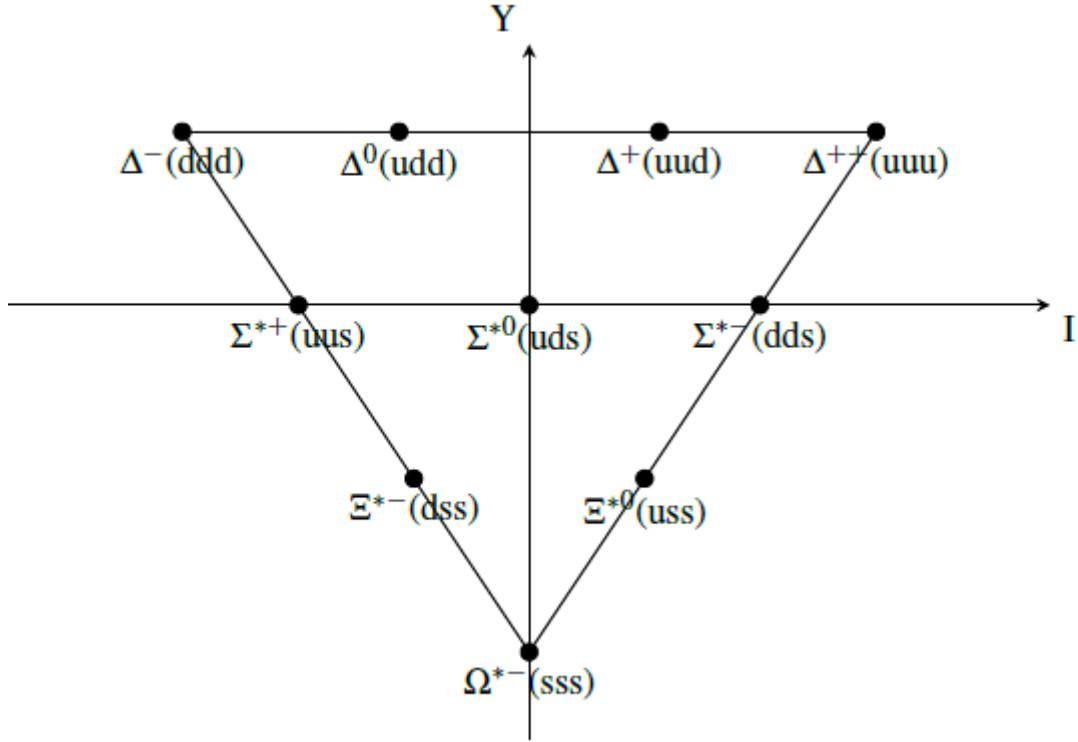


Figure 3.2 Multiplet for  $s-\frac{3}{2}$  baryon decuplet [5]

Spectroscopy of charmed baryons gives us a ground for understanding the dynamics of the light quark sector in environment heavy quark sector [20]. Since 1975, 18 of charmed baryons have been observed and there are four charmed baryons candidate which were not confirmed.

In 1975, the first charmed baryon  $\Lambda_c^+(udc)$  was observed [21]. Its mass was measured as 2286.46(14) MeV by BaBar [22]. This particle was observed with two different methods as fixed target experiment and  $e^+e^-$  experiments by different collaborations.

In this thesis we considered  $\Lambda_c$  and  $\Sigma_c$  baryons that have same quark content. But their flavor wavefunctions are different from each other. Furthermore,  $\Sigma_c$  is an isospin 1 particle. It means that there are three  $\Sigma_c$  particles. Because of the resolution problem of detectors, firstly, doubly charged  $\Sigma_c$  was observed in around 1987. Then singly charged one was observed in 1993 by CLEO [23]. All 18 charmed baryons and decay channels are shown in the Figure 3.3 [24].

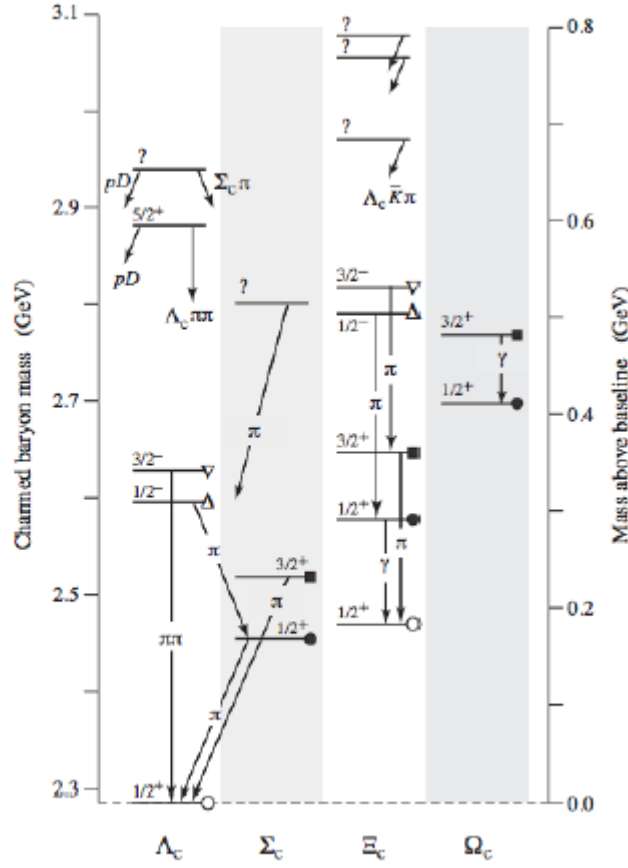


Figure 3.3 Experimentally observed charmed baryons and decay channels [5].

There are eighteen charmed baryons which were observed. Four of them ( $\Lambda_c$ ,  $\Sigma_c$ ,  $\Omega_c$ ,  $\Xi_c$ ) are waiting to be confirmed. In group theory, for  $SU(4)$  group, there must be  $4 \otimes 4 \otimes 4 = 20 \oplus 20 \oplus 20 \oplus 4 = 64$  baryons. In addition, we can classify charmed baryons according to their spin and flavor as we did in light baryons. But now, there is a charm quark besides  $u$ ,  $d$ , and  $s$  light quarks. So these are called  $SU(4)$  multiplets (Fig. 3.4). For having  $s = \frac{1}{2}$  particles, the bottom layer of 20-plet is an  $SU(3)$  octet. 4-plet, an inverted tetrahedron are also  $s = \frac{1}{2}$  baryons (Fig. 3.5). Moreover, for  $s = \frac{3}{2}$  baryons (Fig. 3.5), the bottom layer of 20-plet is a  $SU(3)$  decuplet. For  $\Lambda_c$  and  $\Sigma_c$  baryons' interpolating fields are given in Table 3.4 .

Baryon	Quark content	Interpolating field
$O_{\Lambda_c^+}$	udc	$\frac{1}{\sqrt{6}}\epsilon_{abc}[2(u_a^T C \gamma_5 d_b)c_c + (u_a^T C \gamma_5 c_b)d_c - (d_a^T C \gamma_5 c_b)u_c]$
$O_{\Sigma_c^+}$	udc	$\frac{1}{\sqrt{2}}\epsilon_{abc}[(u_a^T C \gamma_5 c_b)d_c + (d_a C \gamma_5 c_b)u_c]$

Table 3.4 Interpolating fields for  $\Lambda_c$  and  $\Sigma_c$  baryons.  $C$  denotes charge conjugation matrix [6].

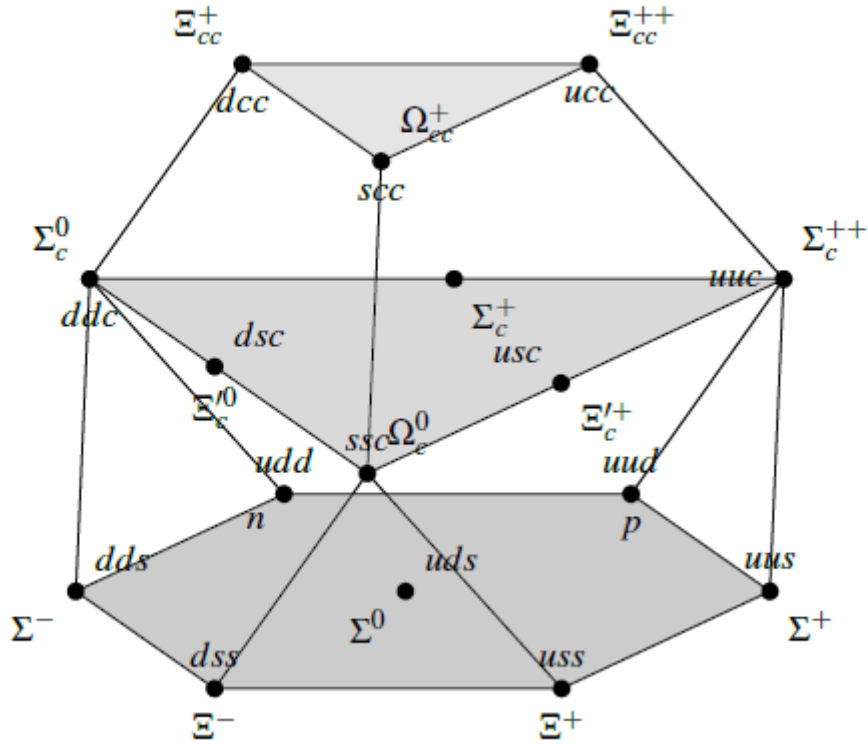


Figure 3.4  $SU(4)$  20-plet for  $s-\frac{1}{2}$  [5].

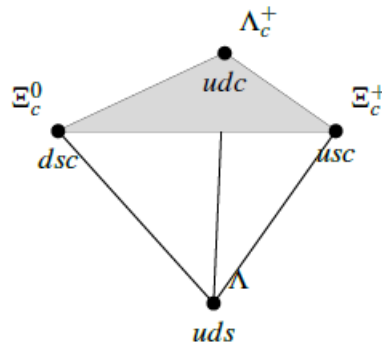


Figure 3.5  $SU(4)$  4-plet for  $s-\frac{1}{2}$  [5].

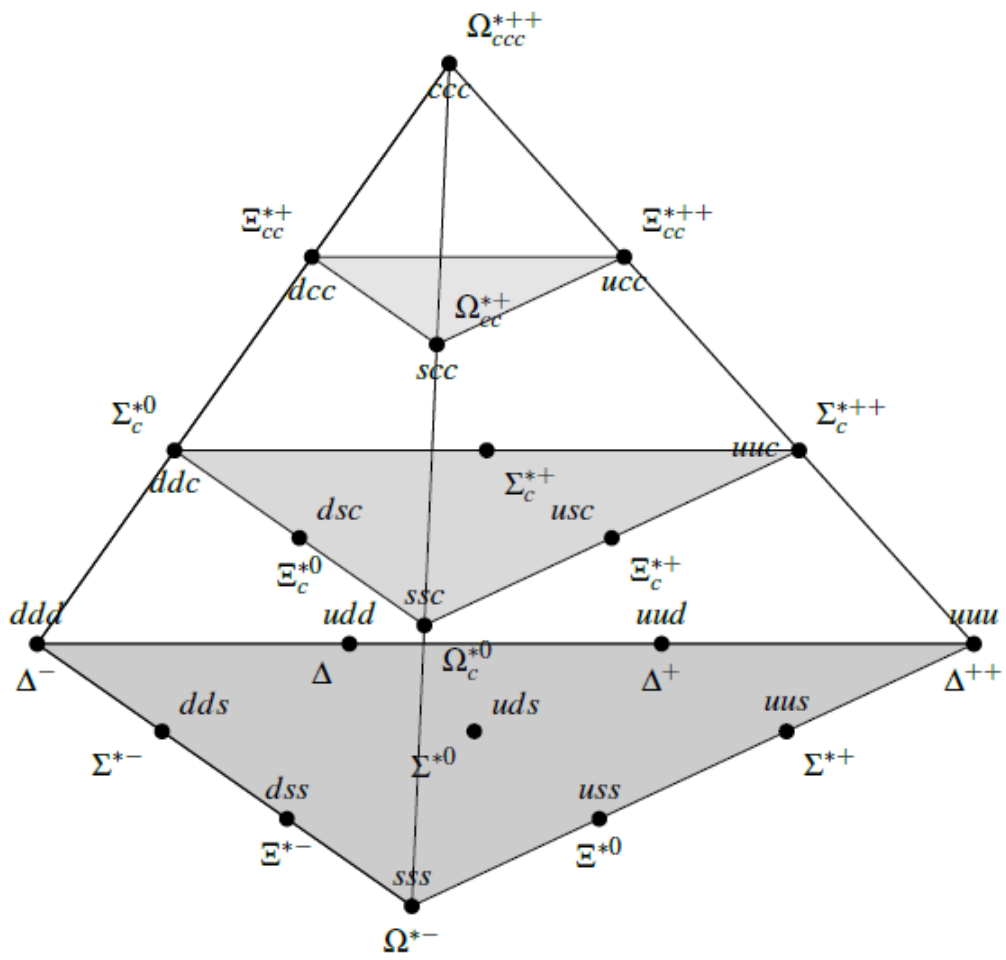


Figure 3.6  $SU(4)$  20-plet for  $s-\frac{3}{2}$  [5].

MASS SPECTRUM AND RESULTS

4.1 Mass Spectrum

After describing the quark propagators as in the previous sections, we use them to obtain the hadron correlators. Then, by using these correlators we can extract the corresponding hadron masses.

Hadron correlation functions' ratios are used to calculate mass spectrum of hadrons  $\Sigma_c$  and  $\Lambda_c$ . So we get a ratio between correlation functions to take an effective mass value ( $m_{eff}$ ) from equation

$$m_{eff}(n_t + \frac{1}{2}) = \ln \frac{C(n_t)}{C(n_t + 1)}. \quad (4.1)$$

When we plot graph by using these mass vs. correlation function relation, it could be seen that the ground state energy dominates the correlator  $C(n_t)$ . So  $m_{eff}$  becomes constant and could be seen an *effective mass plateau* at  $m_{eff} = E_0$ .

Because of that ratio values have tendency to stay constant according to time, we can get fitted mass values by using these *plateaus* as in following  $m_{eff}$  vs *time* graphs and the corresponding fitted results are given in following graphs and tables.

In the following plots, *effective mass plateaus* are plotted in different  $n_t$  ranges in which excited state contributions can be neglected and we can take simple form

$$C(n_t) = A_0 e^{-n_t E_0},$$

$$C(n_t + 1) = A_0 e^{-(n_t+1)E_0}.$$

In the following figures, *plateau* ranges have been drawn with a line. We can find  $m_{eff}$  values in lattice units from this plateau. Moreover, converted values are shown in tables in GeV units.

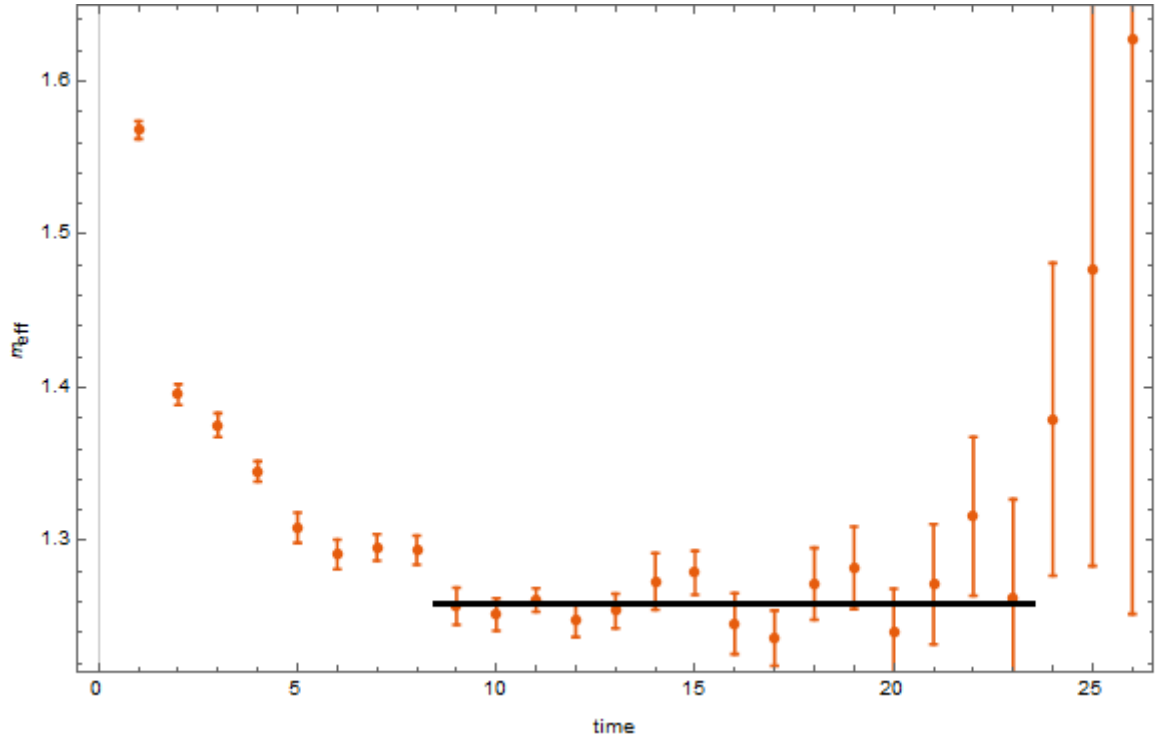


Figure 4.1 Effective mass vs. time graph of  $\Lambda_c$  for  $\kappa = 0.13700$

It can be seen from the Fig. (4.1) that; between 9 and 24 in time, it shows the plateau behavior for  $\Lambda_c$ . So we chose this interval to estimate ground state mass for  $\kappa = 0.13700$ .

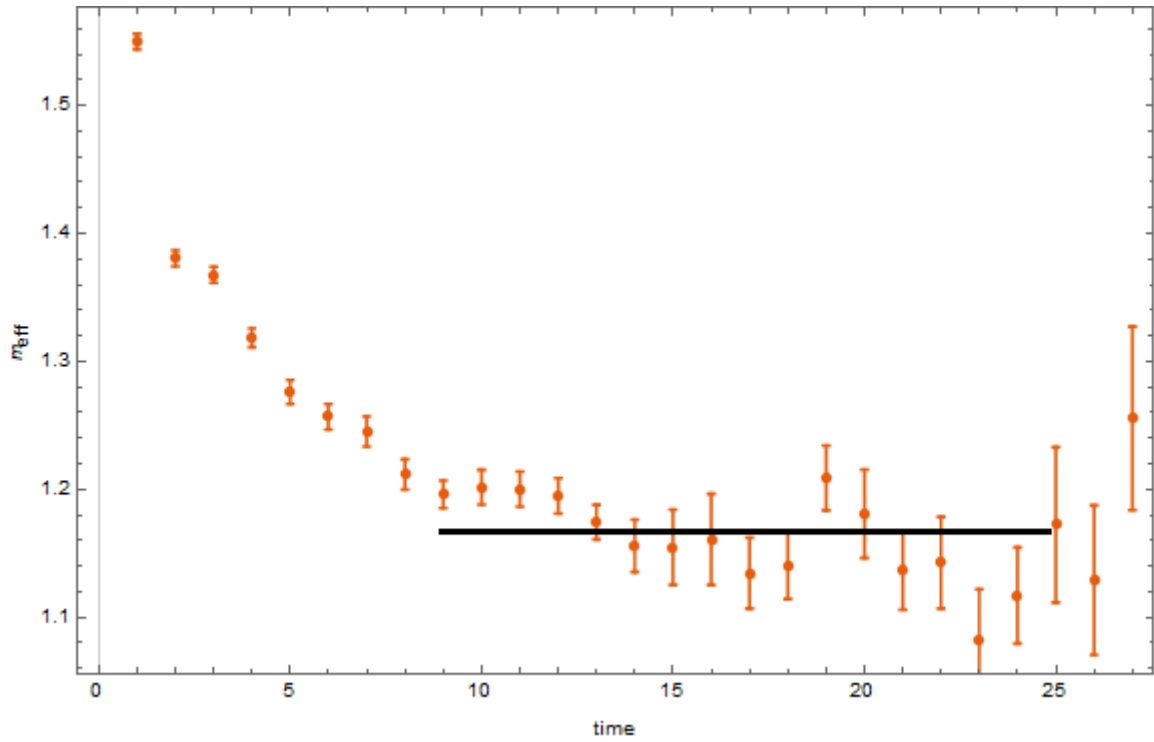


Figure 4.2 Effective mass vs. time graph of  $\Lambda_c$  for  $\kappa = 0.13727$

In Fig. (4.2), we plotted *the effective mass to time* dependence graph for  $\Lambda_c$ . This figure depicts that a plateau region between 9 and 24 is reached for  $\kappa = 0.13727$ .

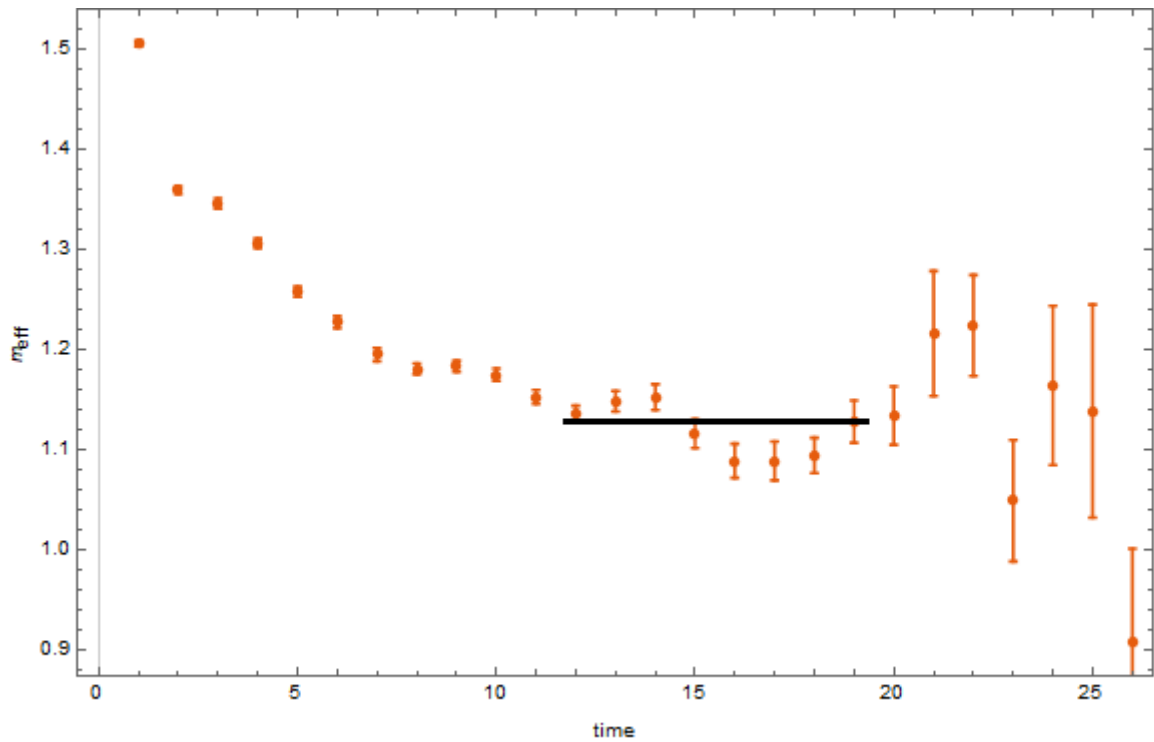


Figure 4.3 Effective mass vs. time graph of  $\Lambda_c$  for  $\kappa = 0.13754$

As shown in Fig. (4.3),  $m_{eff}$  vs.  $time$  graph for  $\Lambda_c$ , we chose time interval between 11 and 17 to show the plateau. It shows ground state values for  $\kappa = 0.13754$ .

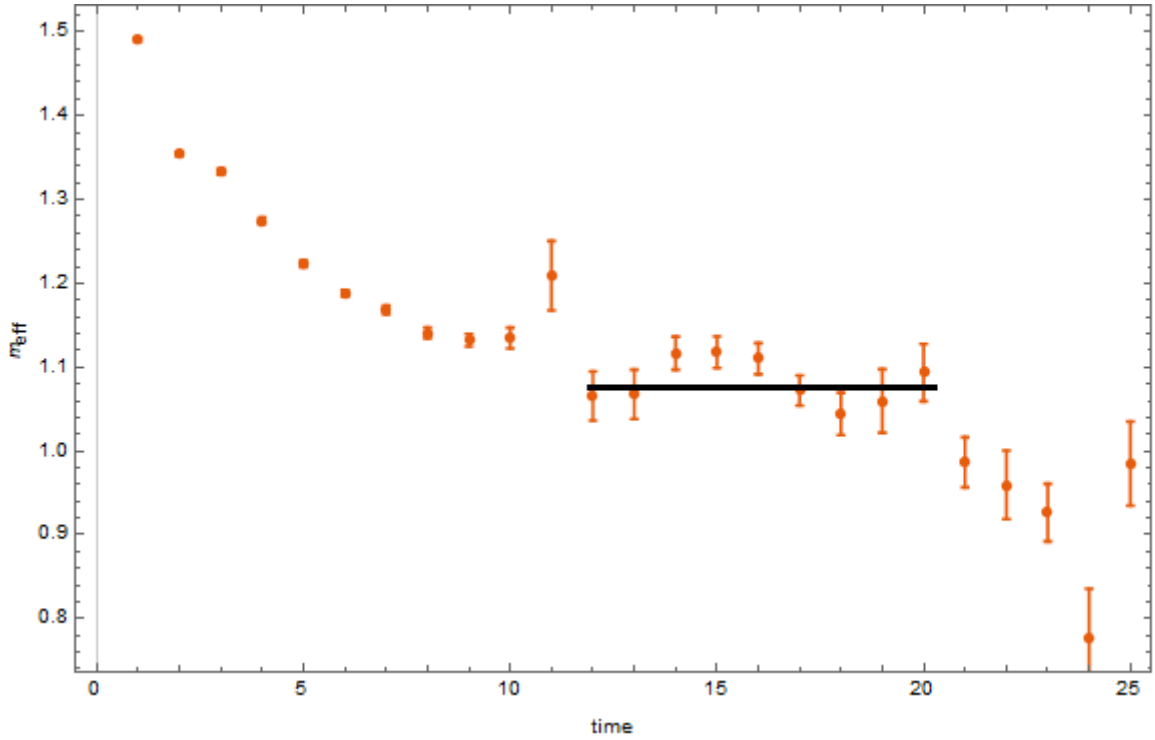


Figure 4.4 Effective mass vs. time graph of  $\Lambda_c$  for  $\kappa = 0.13770$

In Fig. (4.4) that  $m_{eff}$  vs.  $time$  graph for  $\Lambda_c$  baryon is presented. We chose time interval between 12 and 20 to depict the plateau and it shows ground state values for  $\kappa = 0.13770$ .

Table 4.1 The effective mass values for baryons in questions ( $\Lambda_c$ ) for four different light quark hopping parameter values

$\kappa_{val}^{u,d}$	0.13700	0.13727	0.13754	0.13770
$M_{\Lambda_c}(\text{Latt})$	$1.270 \pm 0.020$	$1.161 \pm 0.009$	$1.126 \pm 0.016$	$1.083 \pm 0.036$
$M_{\Lambda_c}(\text{GeV})$	$2.765 \pm 0.045$	$2.527 \pm 0.019$	$2.450 \pm 0.034$	$2.356 \pm 0.080$

Table 4.2 Extrapolated values to chiral limit ( $m_\pi^2 \rightarrow 0$ ) and compared values with other collaborations for  $\Lambda_c$

Chiral Point	This Work	PACS-CS [25]	ETMC [6]
$M_{\Lambda_c}$	$2.268 \pm 0.051$	$2.333 \pm 0.122$	$2.286 \pm 0.027$
Chiral Point	Briceno <i>et al.</i> [26]	Can <i>et al.</i> [27]	Exp. [28]
$M_{\Lambda_c}$	$2.291 \pm 0.066$	$2.412 \pm 0.015$	$2.286 \pm 0.001$

Because of technical disadvantages, we are forced to use unphysical quark masses than physical one. In order to determine the effective masses, we used extrapolation method for our results from physical point to chiral point which means quark mass goes to zero in this limit value ( $m_q \rightarrow 0$ ).

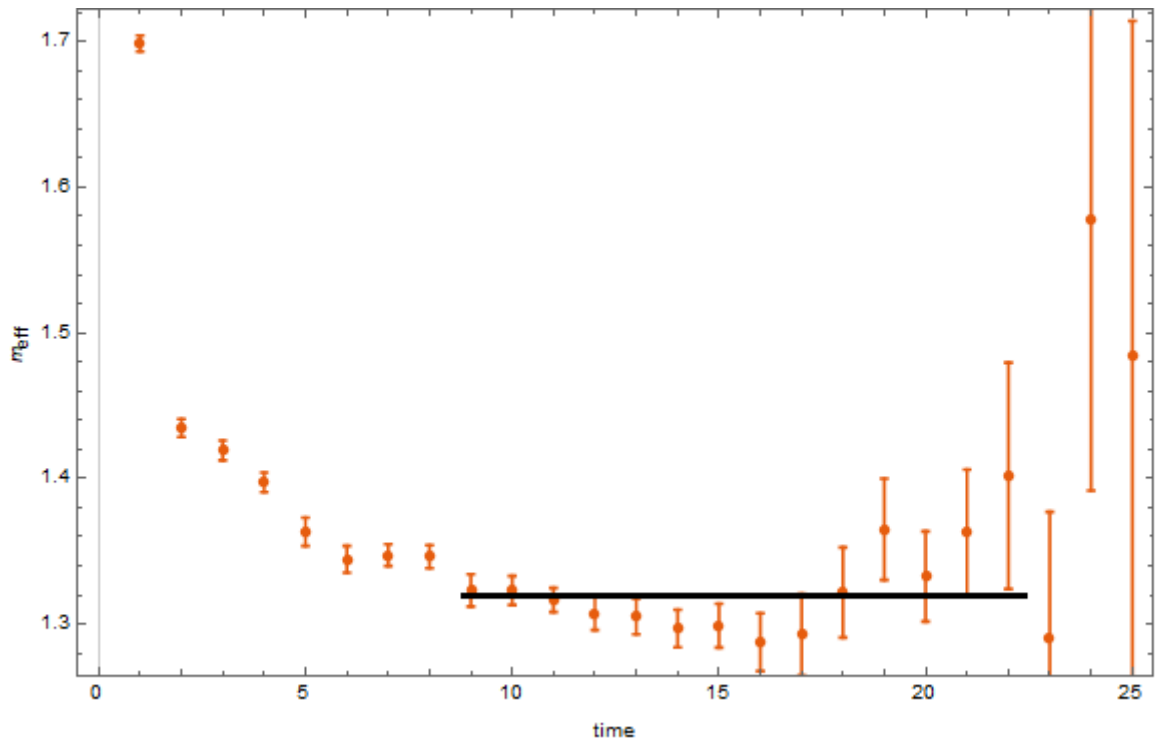


Figure 4.5 Effective mass vs. time graph of  $\Sigma_c$  for  $\kappa = 0.13700$

It can be seen from the Fig. (4.5) that; between 9 and 22 in time, the it shows the plateau behavior for  $\Sigma_c$ . So we chose this interval to estimate ground state mass for  $\kappa = 0.13700$ .

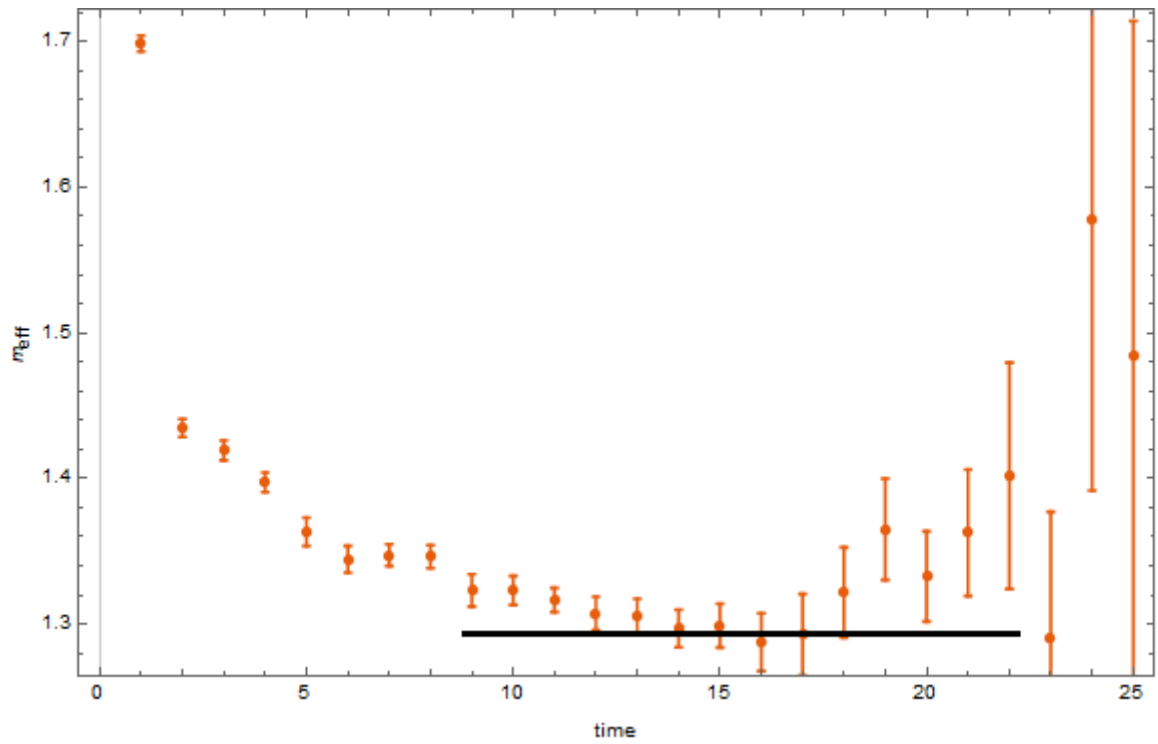


Figure 4.6 Effective mass vs. time graph of  $\Sigma_c$  for  $\kappa = 0.13727$

In Fig. (4.6), we plotted *the effective mass to time* dependence graph for  $\Sigma_c$ . This figure depicts that we chose plateau region between 9 and 22 to exhibit the ground state vicinity and *effective mass* for  $\kappa = 0.13727$ .

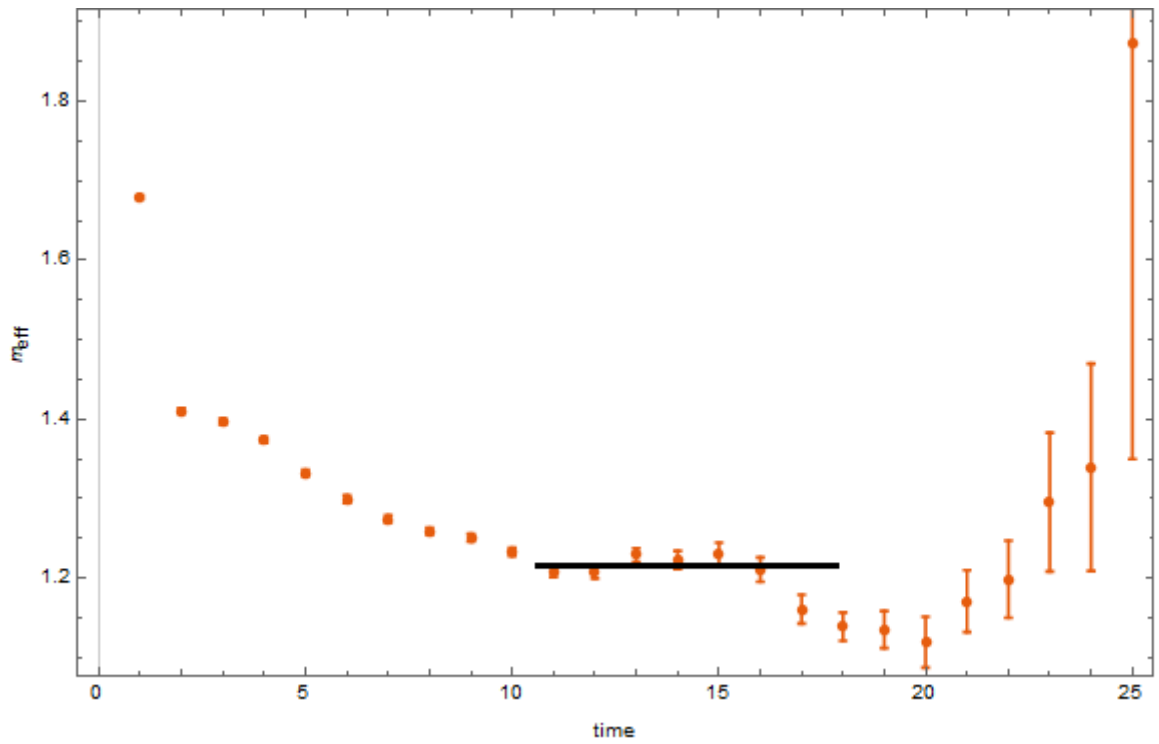


Figure 4.7 Effective mass vs. time graph of  $\Sigma_c$  for  $\kappa = 0.13754$

As shown in Fig. (4.7),  $m_{eff}$  vs.  $time$  graph for  $\Sigma_c$  baryon, we chose time interval between 11 and 17 to show the plateau. It shows ground state values for  $\kappa = 0.13754$ .

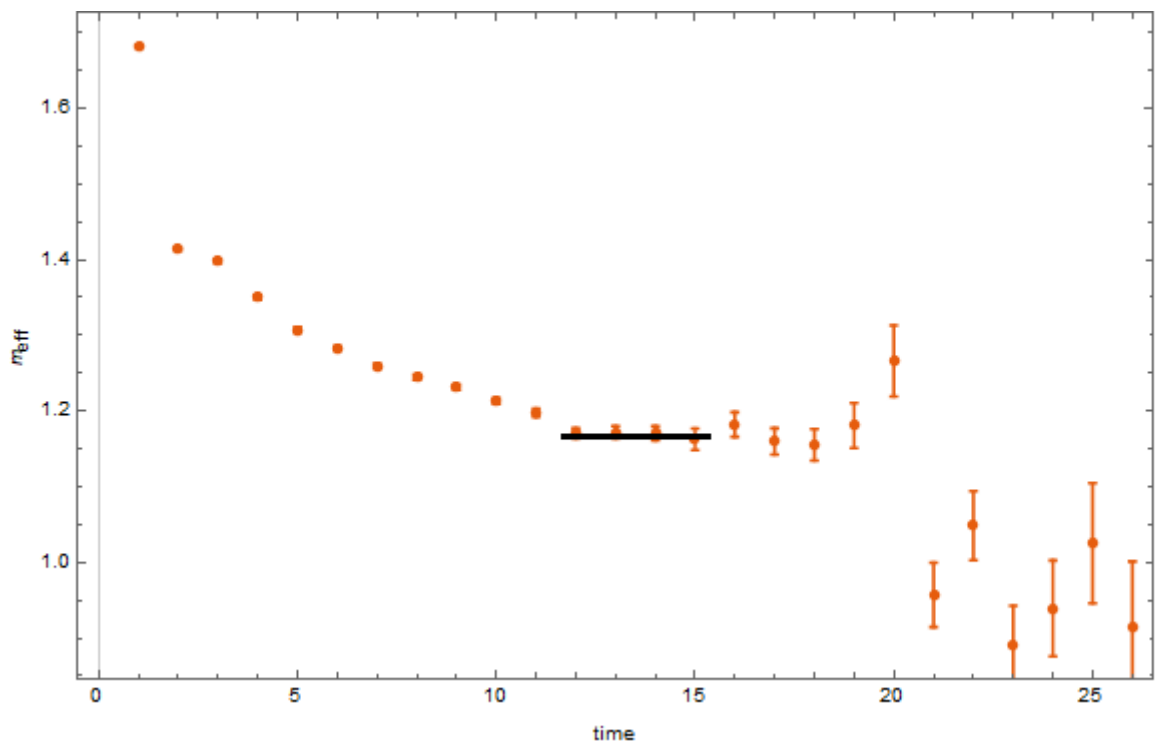


Figure 4.8 Effective mass vs. time graph of  $\Sigma_c$  for  $\kappa = 0.13770$

It is presented in Fig. (4.8) that  $m_{eff}$  vs.  $time$  graph for  $\Sigma_c$  baryon, we chose time interval between 12 and 15 to depict the plateau and it shows ground state values for  $\kappa = 0.13770$ .

Additionally, when we look at the graphs which are shown above corresponding to four hopping parameters, we observe that plateaus in effective mass plots for  $\Lambda_c$  are shorter and noisier as compared to those for  $\Sigma_c$ . Because of flavor content of interpolating fields for particles in question, there are more fluctuation on  $\Lambda_c$  particle's plateau regions than  $\Sigma_c$  ones. A similar behavior can also be observed in the case of octet  $\Sigma$  and  $\Lambda$  baryons [19].

Table 4.3 The effective mass values for baryons in questions ( $\Sigma_c$ ) for four different light quark hopping parameters

$\kappa_{val}^{u,d}$	0.13700	0.13727	0.13754	0.13770
$M_{\Sigma_c}$ (Latt)	$1.324 \pm 0.019$	$1.224 \pm 0.013$	$1.210 \pm 0.014$	$1.168 \pm 0.018$
$M_{\Sigma_c}$ (GeV)	$2.881 \pm 0.042$	$2.663 \pm 0.030$	$2.633 \pm 0.032$	2.543.040

Table 4.4 Extrapolated values to chiral limit ( $m_\pi^2 \rightarrow 0$ ) and compared values with other collaborations for  $\Sigma_c$

Chiral Point	This Work	PACS-CS [25]	ETMC [6]
$M_{\Sigma_c}$	$2.474 \pm 0.031$	$2.467 \pm 0.050$	$2.460 \pm 0.046$
Chiral Point	Briceno <i>et al.</i> [26]	Can <i>et al.</i> [27]	Exp. [28]
$M_{\Sigma_c}$	$2.481 \pm 0.004$	$2.549 \pm 0.072$	$2.453 \pm 0.001$

Also we can fit them to a quadratic function,

$$m_{eff} = a_1 + a_2(am_\pi)^2 + a_3(am_\pi)^4$$

Finally, two different fit results are given in Table 4.3.

Table 4.5 Linear and quadratic extrapolation values

$\chi^2 - fit$	Linear fit	Quadratic fit
Effective mass for $\Lambda_c$	$2.268 \pm 0.051$	$2.346 \pm 0.109$

As it was stated before, we applied again linear and quadratic fit to our resultant data. So we obtained effective mass values for two different kind of fit as in Table 4.6.

Table 4.6 Linear and quadratic extrapolation values

$\chi^2 - fit$	<i>Linear fit</i>	<i>Quadratic fit</i>
<i>Effective mass for <math>\Sigma_c</math></i>	$2.474 \pm 0.031$	$2.558 \pm 0.067$



RESULTS AND DISCUSSION

In this thesis we studied mass spectrum of  $\Lambda_c$  and  $\Sigma_c$  charmed baryons by employing *Lattice QCD* method.

Throughout this work we discussed discretization of continuum space. Then we explained discretization procedure, the plaquette and link variable expressions were shown to provide gauge invariance. Besides, we derived correlation function expression to extract the mass spectrum of particles

$$C(n_t) \equiv \langle \tilde{O}(\mathbf{0}, n_t) \bar{O}(\mathbf{0}, 0) \rangle = \sum_k \langle 0 | \hat{O} | k \rangle \langle k | \hat{O}^\dagger | 0 \rangle e^{-n_t E_k},$$

and finally to extract the effective mass value using

$$m_{eff}(n_t + \frac{1}{2}) = \ln \frac{C(n_t)}{C(n_t + 1)}.$$

The numerical calculation part was done by using an analysis technique to eliminate the bias. The simulations were executed on  $32^3 \times 64$  sized lattice with lattice spacing  $a = 0.0907(13)$  fm ( $a^{-1} = 2.176(31)$ ) GeV and  $N_f = 2 + 1$  dynamical quarks. All calculations were done on four different hopping parameters (gauge configurations) for light quark hopping parameters  $\kappa_{sea}^{u,d} = 0.13700, 0.13727, 0.13754, 0.13770$  which conform to pion masses respectively 700, 570, 410, 300 MeV.

Eventually, we estimated effective mass values of  $\Lambda_c$  and  $\Sigma_c$  by using *Chiral extrapolation* as

$$M_{\Lambda_c} = 2.268 \pm 0.051 \text{ GeV},$$

$$M_{\Sigma_c} = 2.474 \pm 0.031 \text{ GeV},$$

which agree with experiment and consistent with other collaborations' results.

In future works, by using these mass spectrum calculations we can investigate electromagnetic form factors of particles which helps to understand the charmed baryon structure.

It will give us more prediction to explain the heavy quark structure and interactions. All calculations were performed with Mathematica version 10.0.



## REFERENCES

---

- [1] Can, K.U., Kusno, A., Mastropas, E.V. and Zanotti, J.M., (2015). “Hadron Structure on the Lattice”, *Lecture Notes in Physics*, 889: 69-105.
- [2] Patrignani, C. and others, (2016). “Review of Particle Physics”, *Chinese Physics*, C40: 100001.
- [3] Gattringer, C. and Lang, C. B., (2009). *Quantum Chromodynamics on the Lattice: An Introductory Presentation*, Springer.
- [4] Griffiths, D., (2008). *Introduction to Elementary Particles*, Weinheim, Germany: Wiley-VCH 454 p, .
- [5] Aoki, S. and others, (2009). “2+1 Flavor Lattice QCD toward the Physical Point”, *Physical Review*, D79: 034503.
- [6] Alexandrou, C., Drach, V., Jansen, K., Kallidonis, C. and Koutsou, G., (2014). “Baryon Spectrum with  $N_f = 2 + 1 + 1$  Twisted Mass Fermions”, *Physical Review*, D90: 074501.
- [7] Alexandrou, C., (2009). “Baryon Structure from Lattice QCD”, *Chinese Physics*, C33: 1093-1101.
- [8] Bali, G.S., (2001). “QCD Forces and Heavy Quark Bound States”, *Physical Reports*, 343: 1-136.
- [9] Day, J.P., (2013). *Approaches to Non-perturbative Problems in Hadron physics*, Graz U., .
- [10] Ioffe, B.L., (2006). “QCD at Low Energies”, *Program of Particle and Nuclear Physics*, 56: 232-277.
- [11] Reinders, L.J., Rubinstein, H. and Yazaki, S., (1985). “Hadron Properties from QCD Sum Rules”, *Physics Reports*, 127: 1.
- [12] Weinberg, S., (1979). “Phenomenological Lagrangians”, *Physica*, A96:327-34.
- [13] Gasser, J. and Leutwyler, H., (1985). “Chiral Perturbation Theory: Expansions in the Mass of the Strange Quark”, *Nuclear Physics*, B250: 465-516.
- [14] Wilson, K.G., (1974). “Confinement of Quarks”, *Physical Review*, D10:2445-2459.

- [15] Wilson, K.G, (1974). “Quark Confinement.”, Conf. Proc., C7406241: 125-147.
- [16] Wilson, K.G., (1974). “Quark Confinement”, Marseille Colloq.,1974:125, 1974.
- [17] Wang, M.-Z., (2016). “Study of Baryon Production at Belle and BaBar”, Nuclear and Particle Physics Proceedings, 273-275: 2091-2096.
- [18] Avery, P. and others, , (1989). “Observation of the Charmed Strange Baryon  $\Xi(c)0$ ”, Physical Review Letters, 62: 863.
- [19] Naik, P., (2016). “Charmed baryons at LHCb”, PoS, CHARM2016: 047.
- [20] Cheng, H.-Y., (2015). “Charmed Baryons Circa 2015”, Frontiers of Physics (Beijing), 10: 101406.
- [21] Cazzoli, E. G., Cnops, A. M., Connolly, P. L., Louttit, R. I., Murtagh, M. J., Palmer, R. B., Samios, N. P., Tso, T. T. and Williams, H. H., (1975). “Evidence for Delta S = - Delta Q Currents or Charmed Baryon Production by Neutrinos”, Physical Review Letters, 34: 1125-1128.
- [22] Aubert, B. and others, , (2005). “A Precision Measurement of the  $\Lambda^+$  Baryon Mass”, Physical Review, D72: 052006.
- [23] Crawford, G. D. and others, , (1993). “Observation of the Charmed Baryon Sigma (c)+ and Measurement of the Isospin Mass Splittings of the Sigma(c)”, Physical Review Letters, 71: 3259-3262.
- [24] Oka, M., Erkol, G. and Takahashi, T. T., (2009). “Recent QCD results on the Strange Hadron Systems”, PoS, CD09: 021.
- [25] Namekawa, Y. and others, , (2013). “Charmed Baryons at the Physical Point in 2+1 Flavor lattice QCD”, Physical Review, D87: 094512.
- [26] Briceno, R. A., Lin, H.-W. and Bolton, D. R., (2012). “Charmed-Baryon Spectroscopy from Lattice QCD with  $N_f = 2 + 1 + 1$  Flavors”, *Physical Review*, D86 : 094504.
- [27] Can, K., Erkol, G., Oka, M. and Takahashi, T. T., (2017). “ $\Lambda_c \Sigma_c \pi$  Coupling and  $\Sigma_c \rightarrow \Lambda_c \pi$  Decay in Lattice QCD”, Physics Letters, B768: 309-316.
- [28] Olive, K. and others, , (2014). “Review of Particle Physics”, Chinese Physics, C38: 090001.

## CURRICULUM VITAE

---

### PERSONAL INFORMATION

**Name Surname** : Fatih ILGIN

**Date of birth and place** : 19.08.1985 İstanbul

**Foreign Languages** : English

**E-Mail** : fatihlgn@gmail.com

### EDUCATION

<b>Degree</b>	<b>Department</b>	<b>University</b>	<b>Date of Graduation</b>
Master	Physics	Yıldız Technical University	2017
Undergraduate	Physics	Yıldız Technical University	2012
High School	Math-Science	Çatalca High School	2004